III. PREPARATION OF ALUMINA-SILICA COMPOSITE ASSISTED BY MECHANO-CHEMICAL TREATMENT

3.1 Introduction

Chapter 2 successfully demonstrated the influence of mechano-chemical treatment on the surface of alumina to obtain activated powder lead to forming green ceramics body for producing non-firing ceramics. Advantage of this process is that the solid-state reaction is activated due to mechanical energy instead of the temperature. It was shown that the chemical reactivity of starting materials could be improved significantly after mechano-chemical treatment [1, 2]. However, one major problem for ceramic industrial is that the long solidification time and low mechanical strength. Many of alumina properties are controlled by structure and stability of its surface. Moreover, additives interact with the surfaces and modify properties of the alumina materials [3, 4]. Based on the aforementioned problems, there is indeed a need to investigate the effect of composition ratio between alumina-silica similarity aluminosilicate in geopolymer [5-7] by mechano-chemical treatment that reduce the solidification time and increasing the mechanical strength [8-10].

In this chapter has shown that mechano-chemical treatment of alumina-silica composites promoted the formation of Al-O-Si bonds, enhancing the homogeneity of the system [11, 12]. The aim of this work is to gain a better understanding the reaction to form alumina-silica composites during mechano-chemical treatment of alumina and silica powders.

3.2 Experimental Procedure

3.2.1 Sample preparation

The starting materials were Al_2O_3 (Al-160SG-4, Showa-denko Co., Japan) of 0.6 μm mean particle size, fine amorphous SiO_2 (Aerosil 200, Degussa AG) of 12 nm mean particle size and KOH pellets (JIS K 8574). Planetary ball mill was used for mechano-chemical treatment of starting material. According to chapter 2, the mechano-chemical treatment at 300 rpm and 60 min bring about higher specific surface area, X-ray amorphous material, physical broadening microstrain and etc., in this section, the mill was rotated at 300 rpm and milling time at 60 min, respectively. The volume ratio of Al_2O_3- SiO_2 was varied ratio from 1-9 to 9-1. After being mixed at 2,000 rpm for 5 min with an electric mixer, the slurry was poured to Teflon mold and kept at room temperature until solidification. After demolding, the ceramic green body was dried at 25°C, 50%RH for 3 days in the steam oven. Although the fineness of Aerosil silica has disadvantage of increasing the water demand, it was chosen for these experiments for the enhanced reactivity expected to result from its amorphous state. Aerosil has a high water demand and generally the mass of added water was approximately equal to the required amount of Aerosil for any given Al_2O_3:SiO_2 ratio [5]. Possible water has loss during mixing resulting from exothermic reaction between the Aerosil-Alumina and KOH.

3.2.2 Energy transfer

In the course of milling treatments, the rate of phase transformation is essentially controlled by the impact energy, E, and the impact frequency, N. As discussion in previous chapter, beyond a threshold, complete periodicity is reached. Under these circumstances, inelastic collisions take place and all kinetic energy at the impact is transferred to the powder trapped between the zirconia ball and the zirconia bowl. It then follows that the impact energy is given by:

$$E = \frac{1}{2} m_b v_{imp}^2$$

Where m_b is the ball mass and v_{imp}, the relative velocity of the ball, is determined by the ball and bowl velocities at the impact. The collision frequency N has been shown to be almost exactly twice the frequency of the bowl motion, i.e. two collisions per cycle occur. The milling intensity, I, and the energy dose, D, are defined as:

$$I = NE = \frac{1}{2} N m_b v_{imp}^2$$

$$D = It = NEt$$

Where t is the milling time. The total energy transferred per unit mass of the powder, i.e. the specific dose, D_m, is then introduced

$$D_m = NEt / m_p$$

With m_p the mass of the powder batch and t the milling time.

3.3 Results and Discussion

In the following discussion, we have defining the sample compositions in terms of volume ratios of Al_2O_3 to SiO_2 (A-S). Alumina-silica composites divided 2 ranges that high silica content (A1S9, A2S8, A3S7, A4S6) and high alumina content (A5S5, A6S4, A7S3, A8S2, A9S1), respectively.

3.3.1 X-ray diffraction (XRD)

The kinetic of phase transformation was follow by wide angle X-ray diffraction (XRD). The XRD patterns for alumina-silica composites after milling and after solidified by mechano-chemical treatment for 300 rpm and 60 min, are shown in figure 3.1 (a) and (b), respectively. All XRD patterns display strong peaks corresponding to aluminium. These aluminium peaks broaden

slightly with reducing of amount of alumina. The formation mechanism of alumina-silica composites involves the energy transfer of planetary ball mill under mechano-chemical conditions. Figure 3.1 (a) observed forming of dialuminium silicate oxide, $Al_2(SiO_4)O$ near (2θ) $30°$ in high silica content range. While, figure 3.3(b) also observed forming of leucite, $K(AlSi_2O_6)$ near (2θ) $30°$. The milling time is too short to allow chemical bonding to develop between the two dissimilar molecules and the compounds remain discrete, but contain alumina-silica composite particles of Al-O-Si resulting from the mechano-chemical treatment, which enhances the short range diffusion of Al^{3+} near the silica/alumina interface with consequent chemical interaction.

(a)
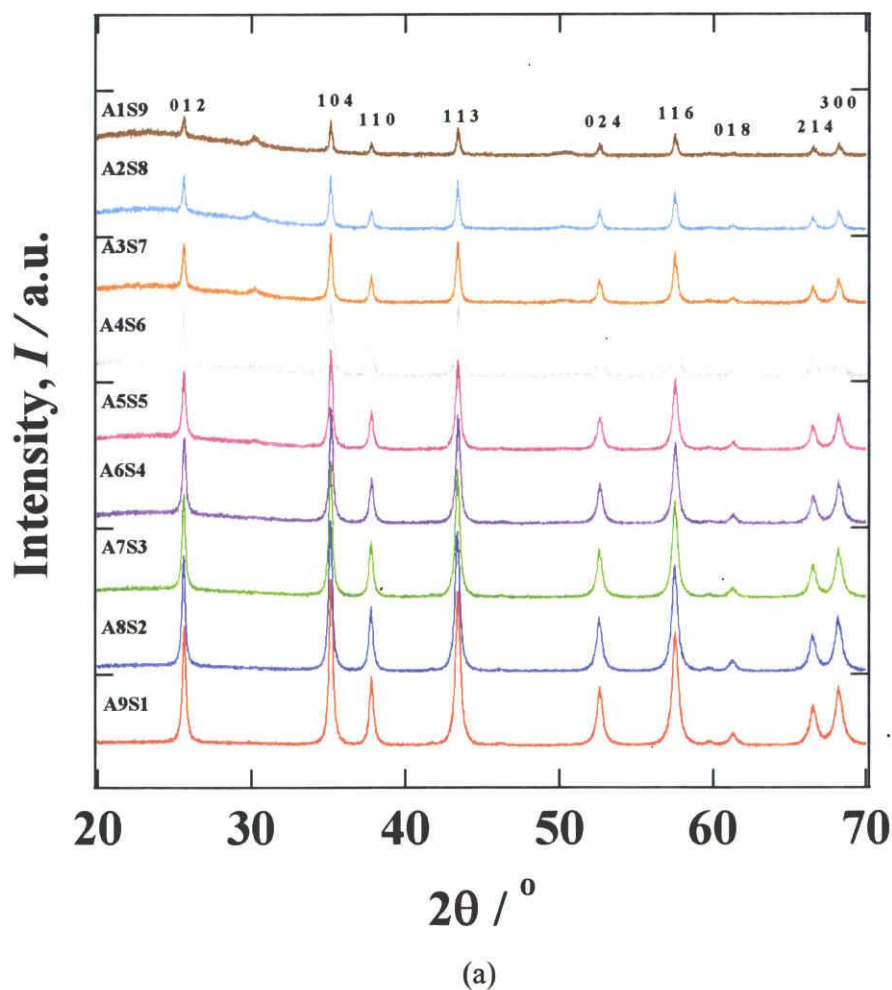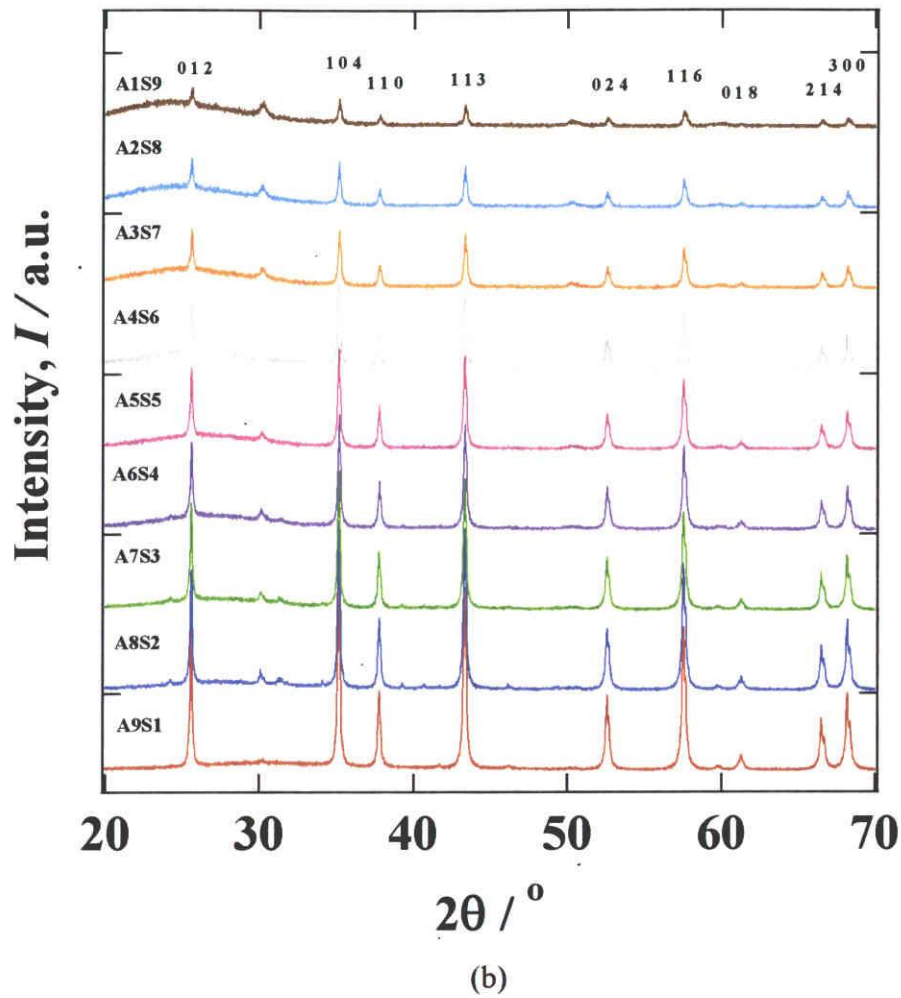
Figure 3.1 XRD patterns of alumina-silica composite by mechano-chemical treatment (300 rpm and 60 min); (a) activated powder, (b) ceramic green body

The energy distribution of the milling process (system) has been calculated in dependence of the amount of material by weight in bowl. The present milling was carried out by planetary ball mill (Pulverisettle 5, Fritsch, Germany). By energy distribution of alumina-silica composites increased with amount of alumina content. Due to energy distribution in planetary ball mill is corresponding to mass ratio of material. The density of alumina is higher than density of silica,

therefore, energy distribution also depending on mass ratio of alumina. Working parameters are summarized in Table 3.1.

Table 3.1 Energy transfer of alumina-silica composites

Conditions A-S	v (rev./min)	N (Hz)	v_{imp} (m.s^{-1})	E (J)	I_M (W.g^{-1})	$t_{1/2}$ (s)	$D_{m,1/2}$ (kJ.g^{-1})
1-9	300	5.00	17.898	0.477	2.387	3600	0.0859
2-8	300	5.00	26.376	1.037	5.183	3600	0.1866
3-7	300	5.00	34.854	1.810	9.050	3600	0.3258
4-6	300	5.00	43.332	2.798	13.989	3600	0.5036
5-5	300	5.00	51.81	4.000	19.998	3600	0.7199
6-4	300	5.00	60.288	5.416	27.078	3600	0.9748
7-3	300	5.00	68.766	7.046	35.229	3600	1.2683
8-2	300	5.00	77.244	8.890	44.451	3600	1.6003
9-1	300	5.00	85.722	10.949	54.745	3600	1.9708

3.3.2 Specific Surface area (BET)

Figure 3.2 shows the change in specific surface area of the alumina-silica composites. When Al-Si composites increase, the specific surface area decreases. The decrease in s_{BET} may cause an increase in the Al-Si contact area attributable to the stuffing of micropores in the aggregates of small particles by mechanical stress introduced by mechano-chemical treatment by milling.
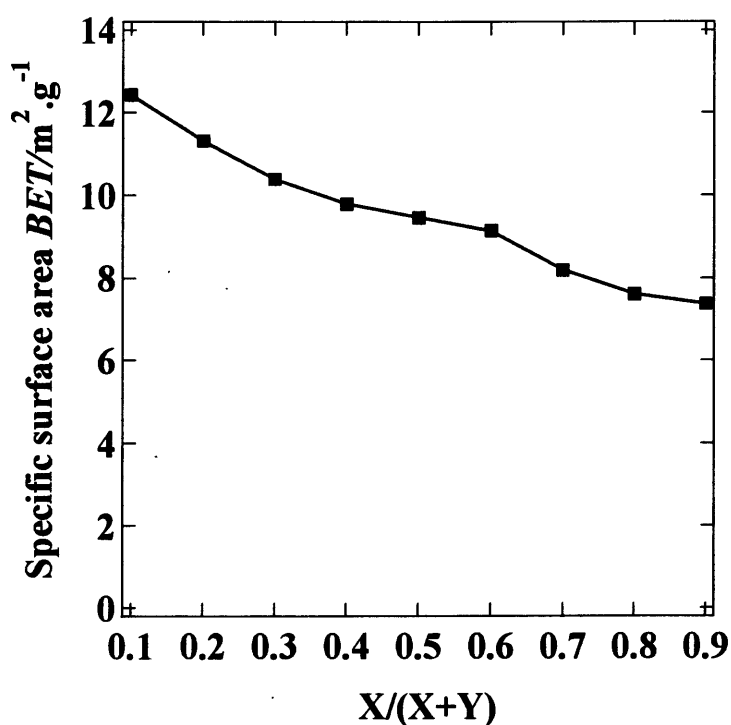
Figure 3.2 Specific surface area of activated alumina-silica composites

3.3.3 ICP analysis

Figure 3.3 shows the elution analysis of the activated alumina-silica composite particles treated by ball milling. It is known that Al^{3+} ion and Si^{4+} ion mainly leached out from ceramic particles, when ceramics particles are mixed with potassium hydroxide solutions. The activated alumina-silica composite particles showed elution of Al^{3+} ion and Si^{4+} ion leaching in the all samples. Al^{3+} ion and Si^{4+} ion contents were decreased with an increasing of alumina content. Due to agglomeration of small particles at high alumina content lead to reducing of BET surface area, the leaching of Al^{3+} ion and Si^{4+} ion also decreased.
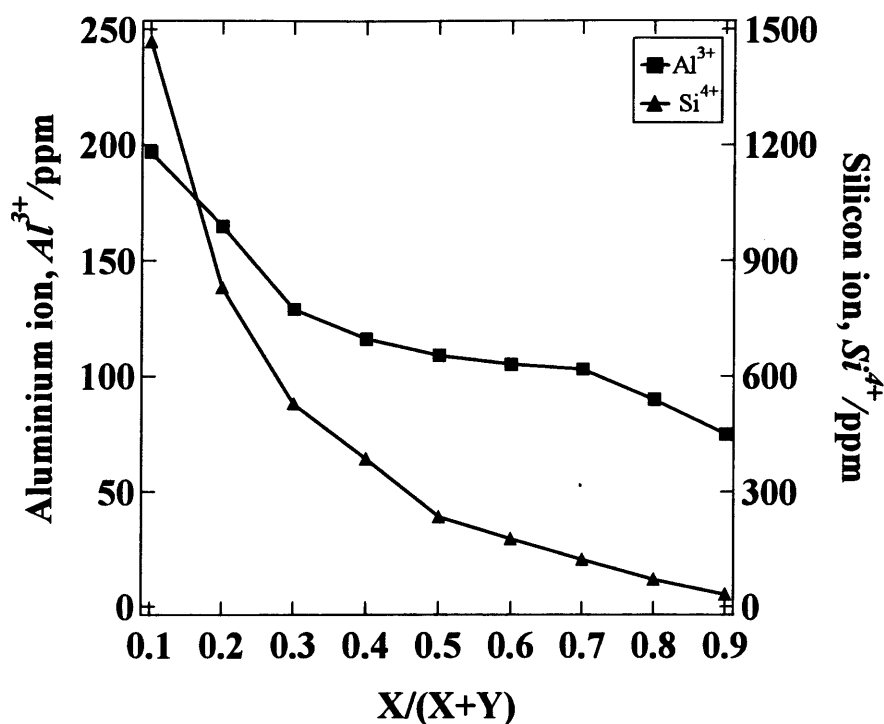
Figure 3.3 Elution behavior of the activated alumina-silica composites;

X = Alumina, Y = Silica

3.3.4 TG-DTA analysis

The thermogravimetric traces, conducted in oxygen atmosphere, for the solidified body formed from alumina-silica composite with mechano-chemical treatment (300 rpm and 60 min) were given in Figure 3.4. The weight loss of composite (a), (b), (c), (d), (e), (f), (g), (h) and (i) are 3.6%, 3.2%, 3.0%, 2.7%, 3.5%, 3.8%, 5.6%, 6.4%, 8.8%, respectively. As previous mentioned, high silica content (composite (a) – composite (d)) and high alumina content (composite (e) – composite (i)). The weight loss of composite (a) greater than composite (b), (c) and (d), respectively in high silica content may be due to the trapping H_2O and CO_2 in the small pores of densely-packed aggregates during mechano-chemical treatment. On the other hand, the weight loss of the high alumina content is greater than for high silica content, composite (i), (h), (g), (f),

(e), respectively. This is because of the mechano-chemical treatment on surface of alumina has a great effect than surface of silica.

For the DTA traces, under the same experimental condition, endothermic peaks and exothermic peaks were observed in all samples. Composite (a) contains endothermic peaks attributed the dehydration of adsorbed water at 51°C and dehydroxylation of small peak at 162°C, and exothermic peak at 340°C and 875°C. Composite (b) contains endothermic peaks attributed the dehydration of adsorbed water at 53°C and dehydroxylation of small peak at 172°C, and exothermic peaks at 340°C and 889°C. Composite (c) contains endothermic peaks attributed the dehydration of adsorbed water at 50°C and exothermic peaks at 338°C. Composite (d) contains endothermic peaks attributed the dehydration of adsorbed water at 54°C and exothermic peaks at 339°C. Composite (e) contains endothermic peaks attributed the dehydration of adsorbed water at 52°C and exothermic peaks at 342°C. Composite (f) contains endothermic peaks attributed the dehydration of adsorbed water at 55°C and dehydroxylation of small peak at 157°C, and exothermic peaks at 343°C and 504°C. Composite (g) contains endothermic peaks attributed the dehydration of adsorbed water at 58°C and dehydroxylation of small peak at 160°C, and exothermic peaks at 342°C. Composite (h) contains endothermic peaks attributed the dehydration of adsorbed water at 61°C and dehydroxylation of small peak at 133°C and 180°C, and exothermic peaks at 338°C. Composite (i) contains endothermic peaks attributed the dehydration of adsorbed water at 62°C and dehydroxylation of small peak at 131°C and 166°C, and exothermic peaks at 334°C. The temperatures tending was decrease slightly with increasing Al_2O_3 content. The endothermic peaks corresponding dehydroxylation of alumina-silica composites was not observed in composite (a) − composite (e) because the Al_2O_3 content in this sample is too low. The endothermic peak of composite (a) is shifted from 51°C to 62°C in composite (i) due to mechano-chemical dehydration and increased adsorption of surface water.

111

On the other hand, total endothermic peaks also increased. This is also agreeing with previous

mention that mecahno-chemical treatment on surface of alumina greater than surface of silica.

The small 875°C exothermic peak in composite (a) and 889 °C exothermic peak in composite (b)

are probably due to the formation of small amount of transition alumina arising from AlO(OH),

which has been reported to form on the surface of Al_2O_3 during milling [13].

(a)

(b)

(c)

113

Weight loss, %

Exothermic   Endothermic

54

339

Temperature, °C

(d)

Weight loss, %

Exothermic   Endothermic

52

342

Temperature, °C

(e)

(f)

(g)

115

(h)

(i)

116
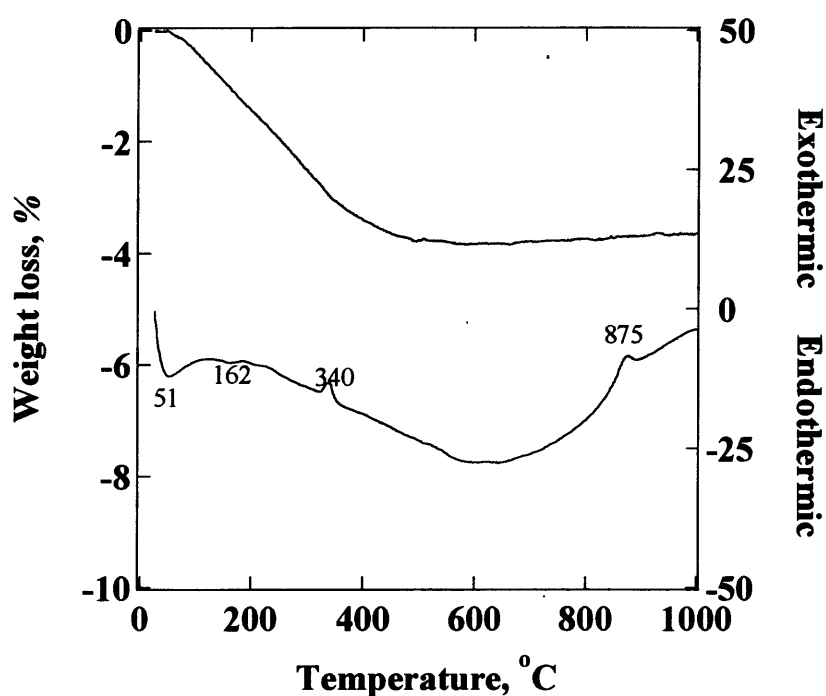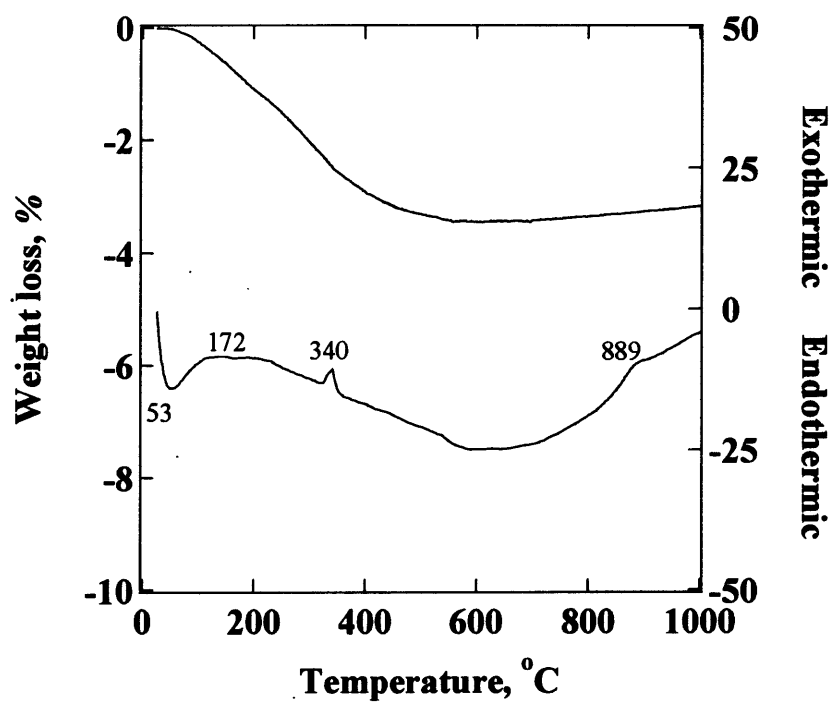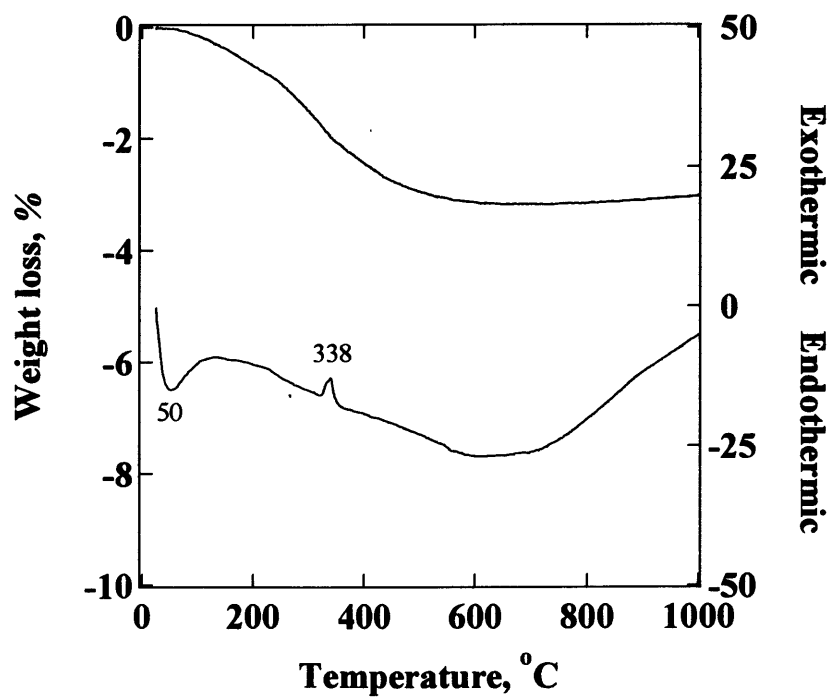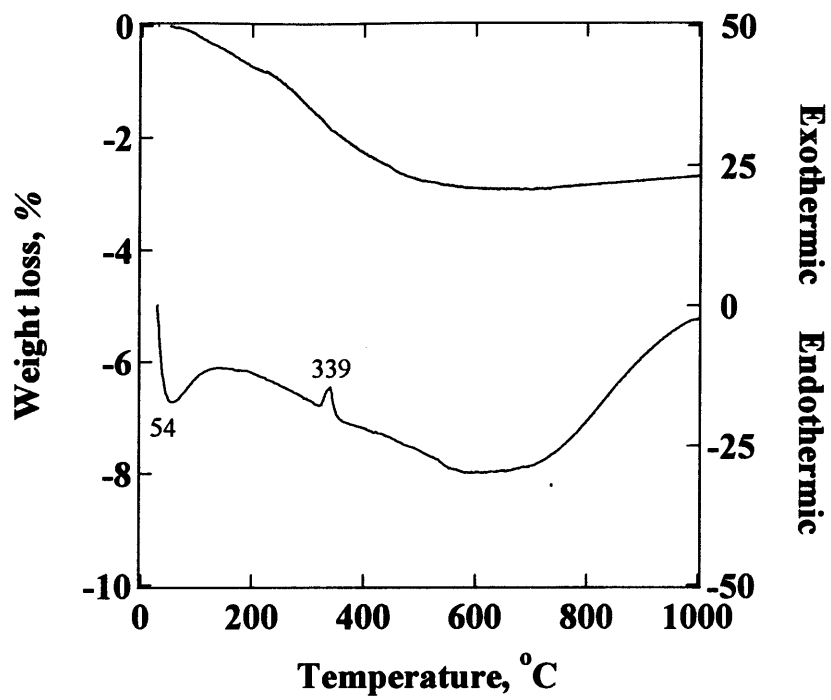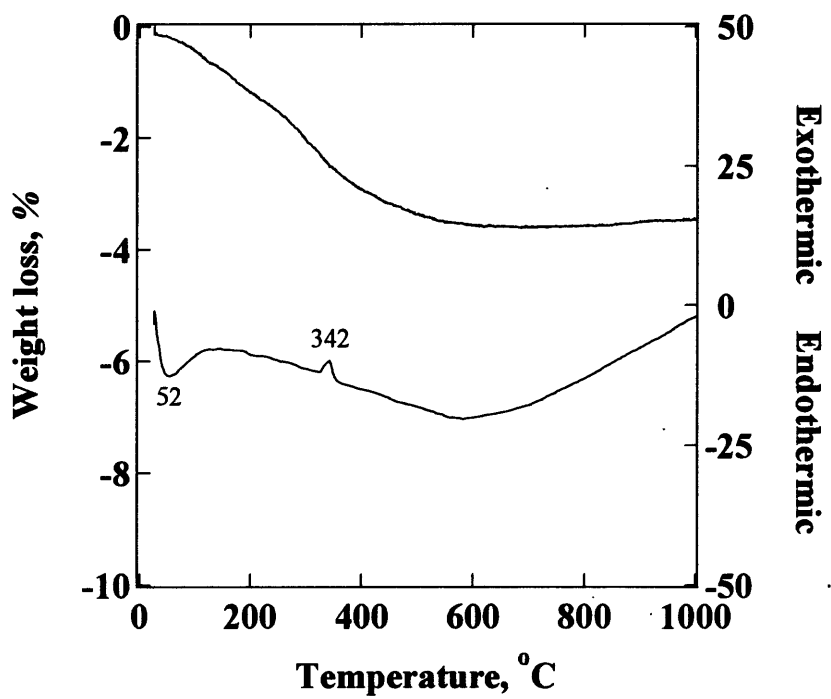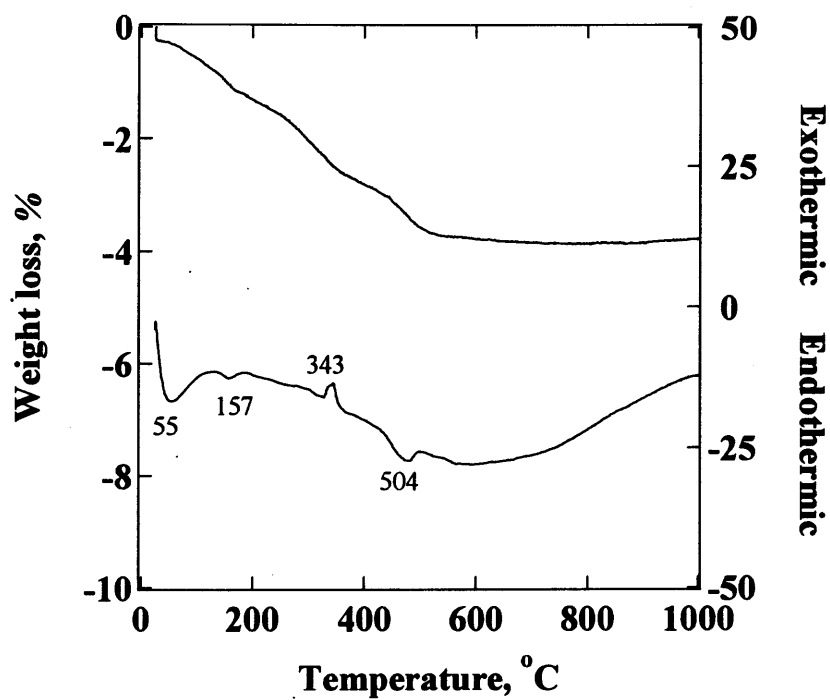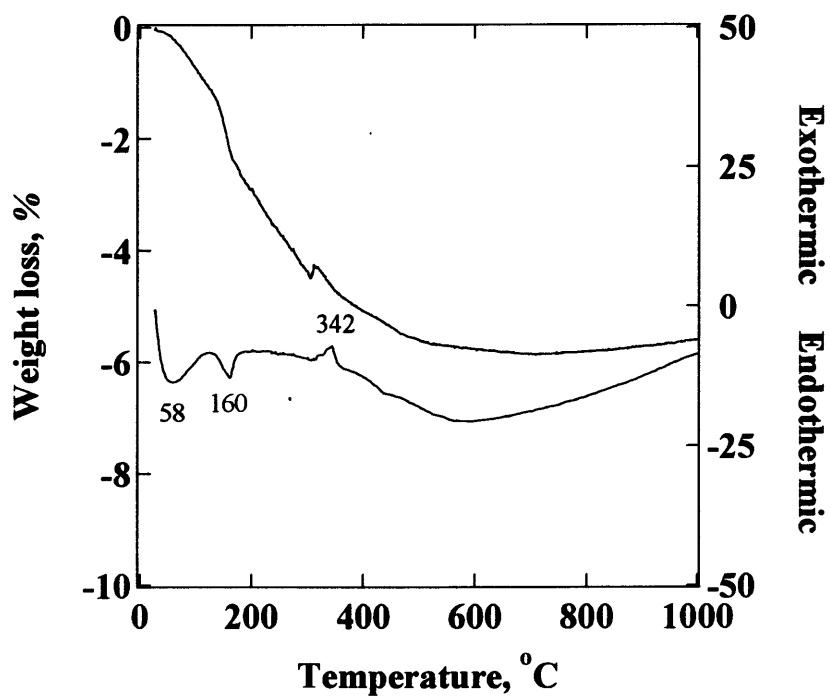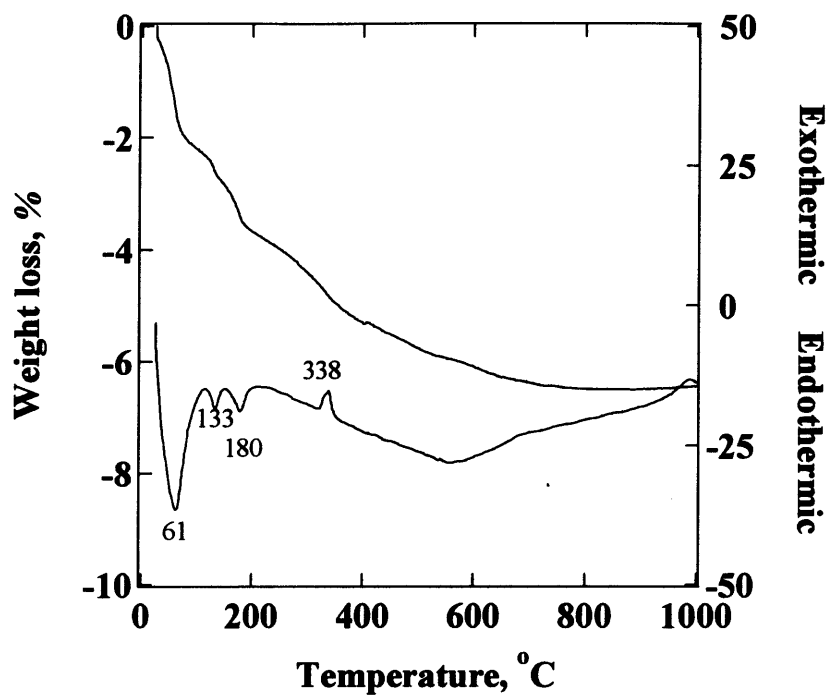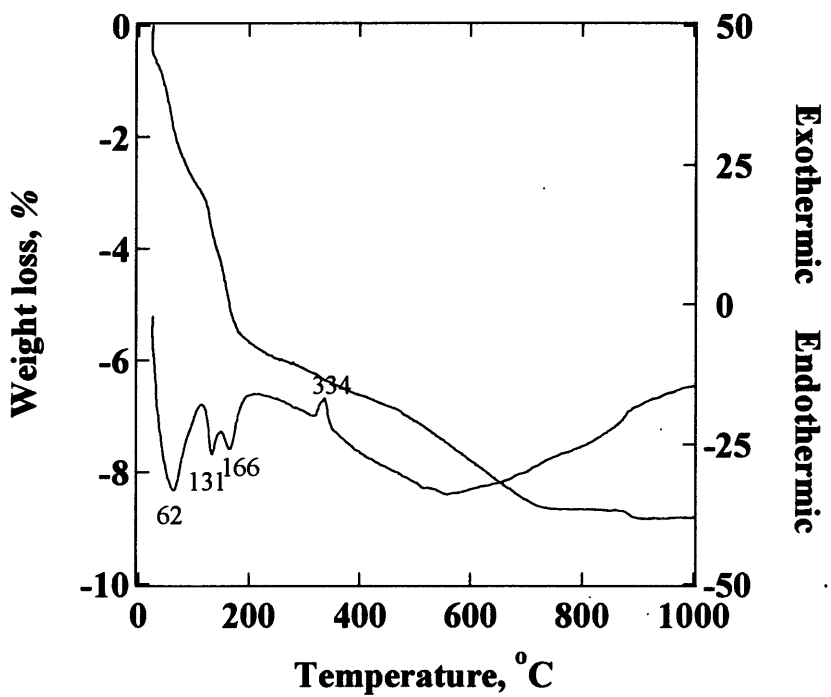
Figure 3.4 TG-DTA of alumina-silica composite by mechano-chemical treatment

(300 rpm and 60 min); (a) A1S9, (b) A2S8, (c) A3S7, (d) A4S6,

(e) A5S5, (f) A6S4, (g) A7S3, (h) A8S2, (i) A9S1

3.3.5 Microstructure and Morphology (FE-SEM)

In order to study the microstructural and morphological changes of samples, the solidified alumina-silica composite of mechano-chemical treatment (ceramic green body) were observed by FE-SEM as shown in figure 3.5. By figure 3.5 (a), (b), (c), (d), (e), (f), (g), (h) and (i) corresponding to solidified alumina-silica composites, A1S9, A2S8, A3S7, A4S6, A5S5, A6S4, A7S3, A8S2 and A9S1, respectively. The microstructure and morphology of each sample were difference and depending on volume ratio of alumina-silica system. As figure 3.5(a), the powder has excess by silica content which's heterogeneous system. The silica content decrease in figure 3.5 (b), 3.5 (c) and 3.5 (d) indicate, the powder has preserved their flake like shape. The surface have homogeneous system in figure 3.5 (e) and 3.5 (f) due to amount of alumina and silica enough for forming in binary system. With increasing alumina content in figure 3.5 (g), 3.5 (h) and 3.5 (i), the clusters become smaller in size. The solidified bodies consisted of the fine alumina grain. Due the non-solidified bodies, it is difficult to facilitate the formation of necks between adjoining alumina-silica composites bindered with alkaline solution (KOH).

(a)

X 3,000   15.0kV SEI   LM   WD 7.9mm   1μm

(b)

X 3,000   15.0kV SEI   LM   WD 8.0mm   1μm

(c)

X 3,000   15.0kV SEI   LM   WD 8.0mm   1μm

(d)

X 3,000   15.0kV SEI   LM   WD 8.0mm   1μm

(e)

X 3,000   15.0kV SEI   LM   WD 8.0mm   1μm

(f)

X 3,000   15.0kV SEI   LM   WD 8.1mm   1μm

(g)

X 3,000   15.0kV SEI   LM   WD 8.1mm   1 μm

(h)

X 3,000   15.0kV SEI   LM   WD 8.1mm   1 μm
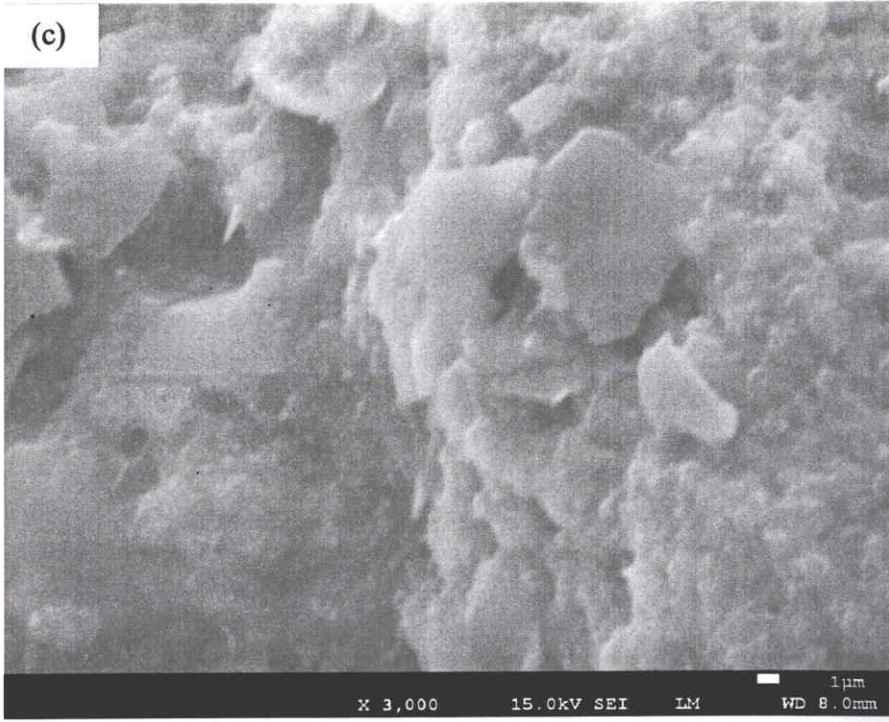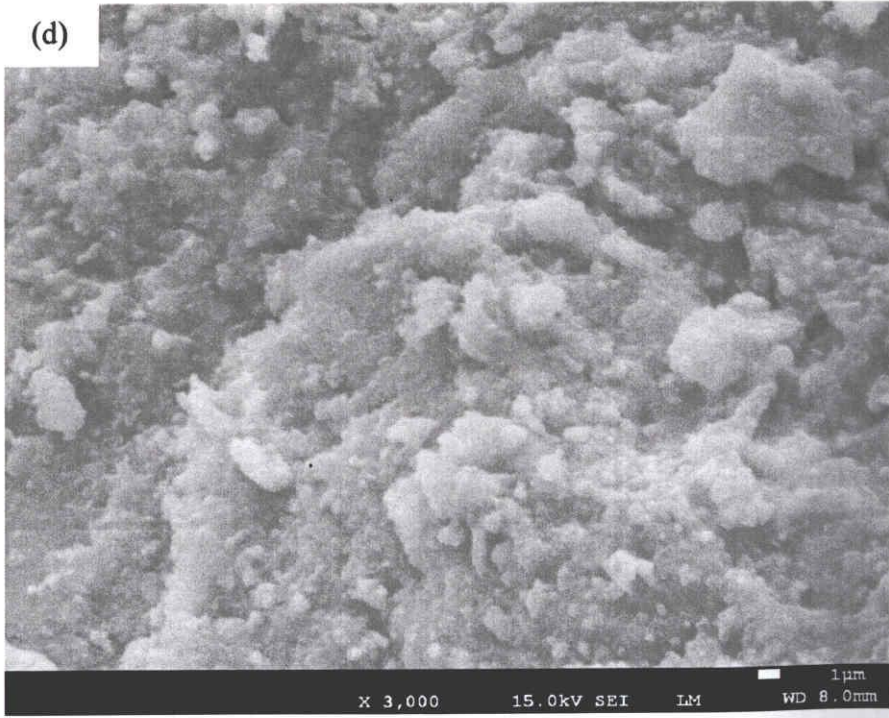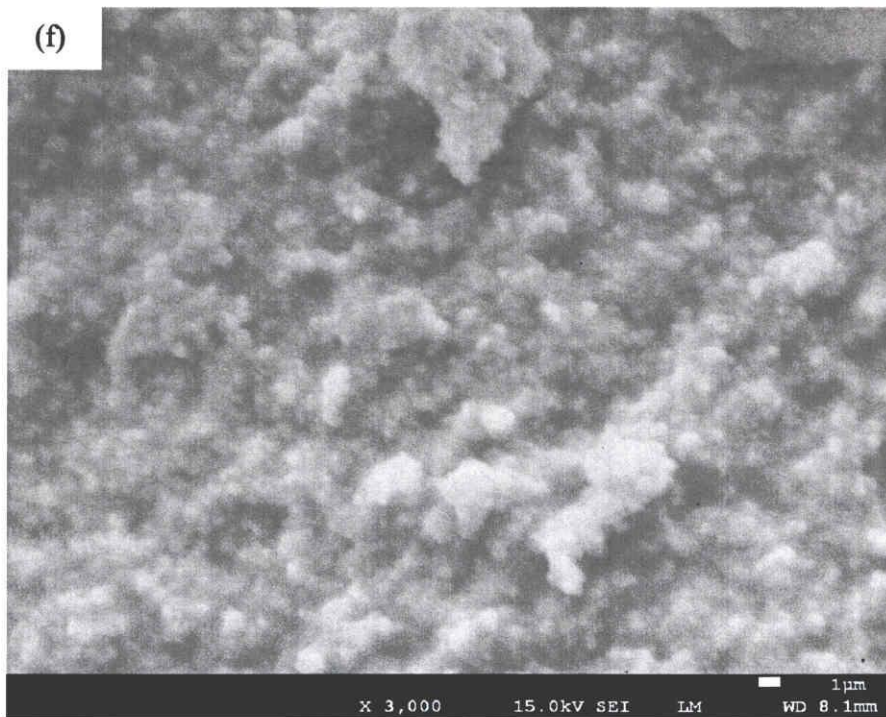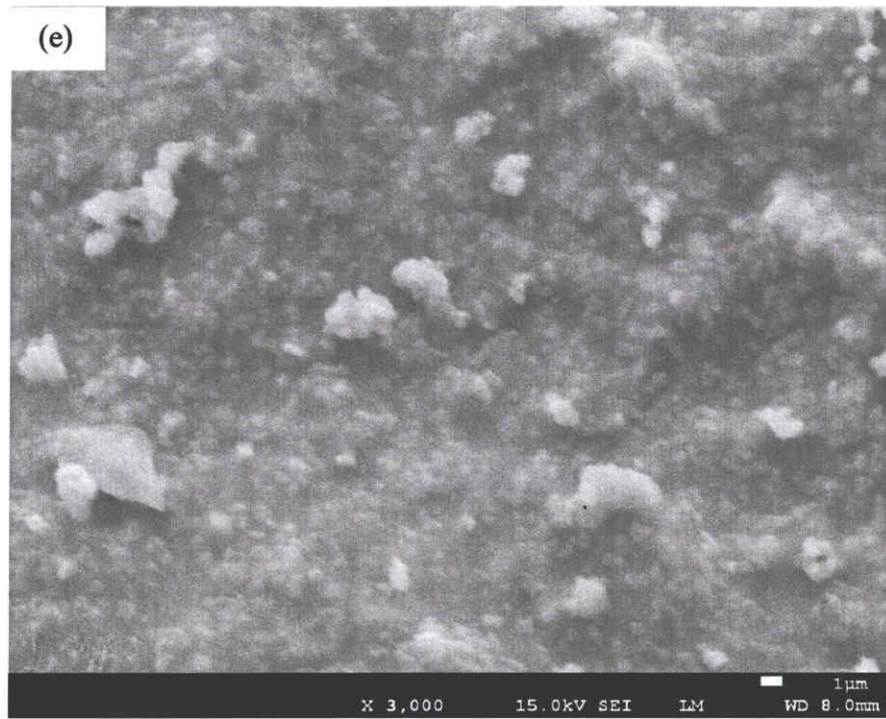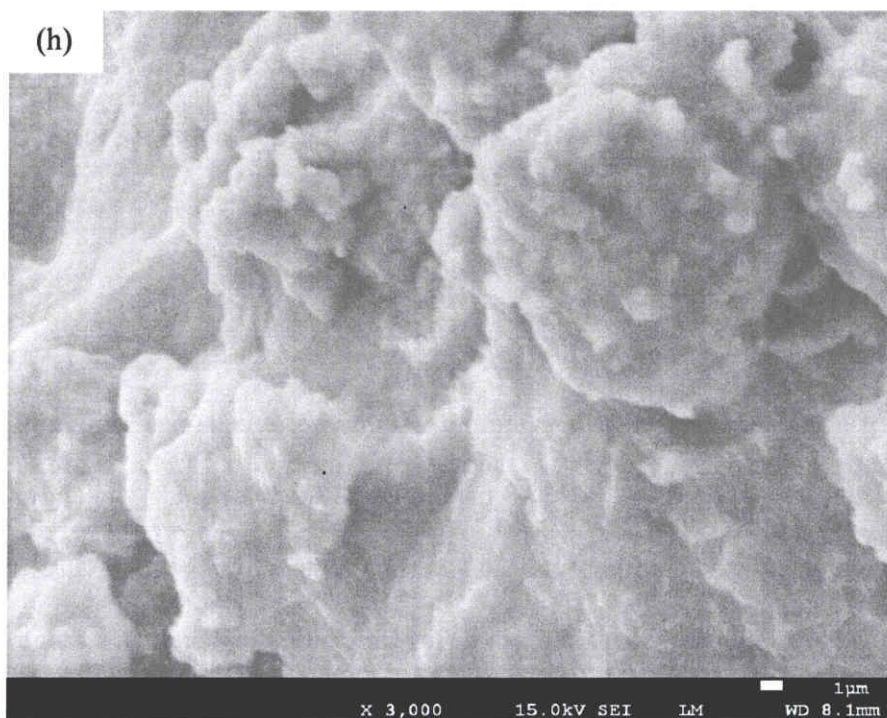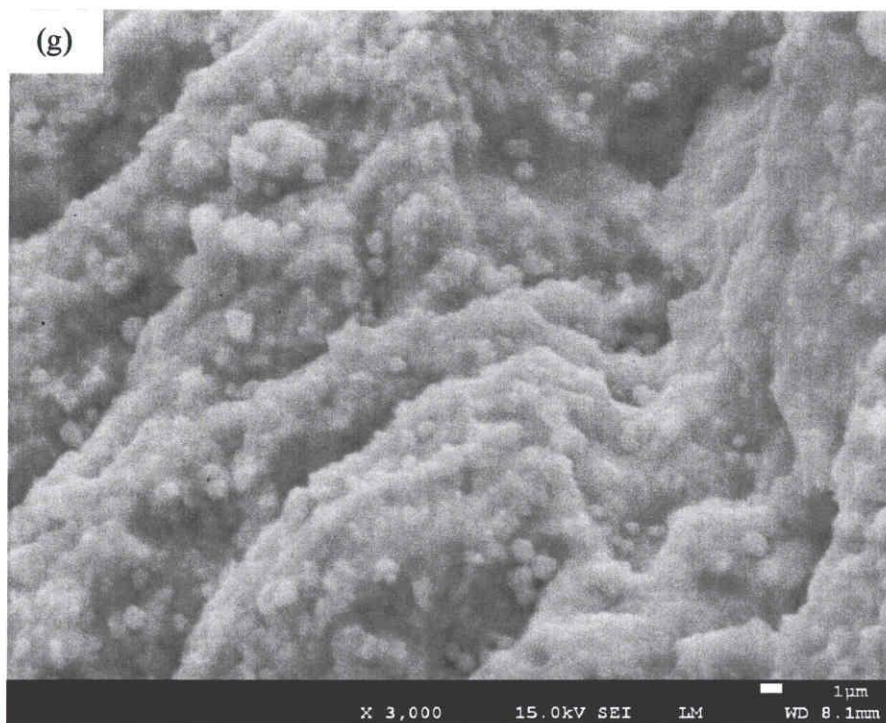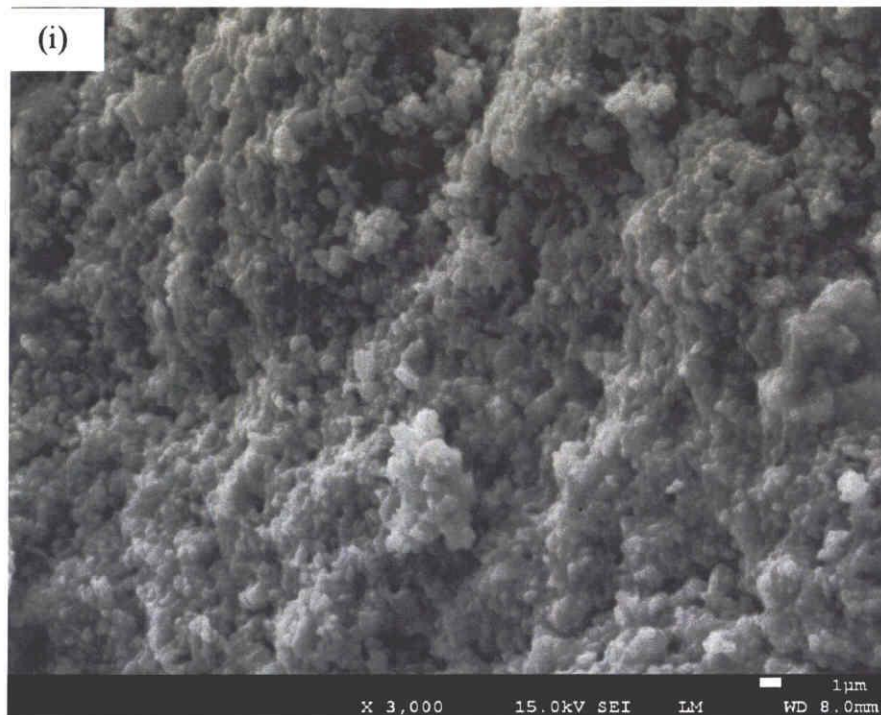
Figure 3.5 Microstructural evolution of solidified alumina-silica composite by mechano-chemical treatment (300 rpm and 60 min); (a) A1S9, (b) A2S8, (c) A3S7, (d) A4S6, (e) A5S5, (f) A6S4, (g) A7S3, (h) A8S2, (i) A9S1.

3.36 *Solidification time and Bending strength*

A production of good quality non-firing ceramic with higher mechanical strength and reduction of solidification time depends on several parameters like kind and concentration of KOH, mechano-chemical condition, curing time and curing temperature, etc. Figure 3.6 represents, which illustrate the relationship between solidification time and bending strength of solidified body at different composition ratio of alumina-silica. It can be divided 2 ranges that high silica content $(X/(X+Y)) = 0.1$-0.4 and high alumina content $(X/(X+Y)) = 0.5$-0.9 as follow. The bending strength increased with decreasing of silica content in high silica content range while decreasing

with increasing of alumina content in high alumina content range. In order to evaluate mechanical properties of samples, bending strength tests were conducted. Consider now issues of composition ratio of Al_2O_3-SiO_2 on bending strength. Increasing amount of SiO_2 was shown to increase bending strength. However, strength behavior can be significantly different from that of SiO_2, which as SiO_2 is maximum when the SiO_2 particles have no stabilizer and easy fracture. Strength of Al_2O_3-SiO_2 composites generally increase with mechano-chemical treatment, similar to, but often less than the relative increases of SiO_2, especially at higher SiO_2 contents, due silica property is more evident than mechano-chemical treatment. This proposed cause of strengths not following the SiO_2 increases due to processing heterogeneities. On the other hand, solidification time was decreased with increasing of silica in high silica content range due to silica (Aerosil) has a high water demand and generally the mass of added water was approximately equal to the required amount of Aerosil in system and also decreases with increasing of alumina in high alumina content range because water has loss during mixing resulting from exothermic reaction between the Aerosil-Alumina and KOH. According to DTA results in figure 3.4, the exothermic reactions have corresponding to alumina content greater than silica content.
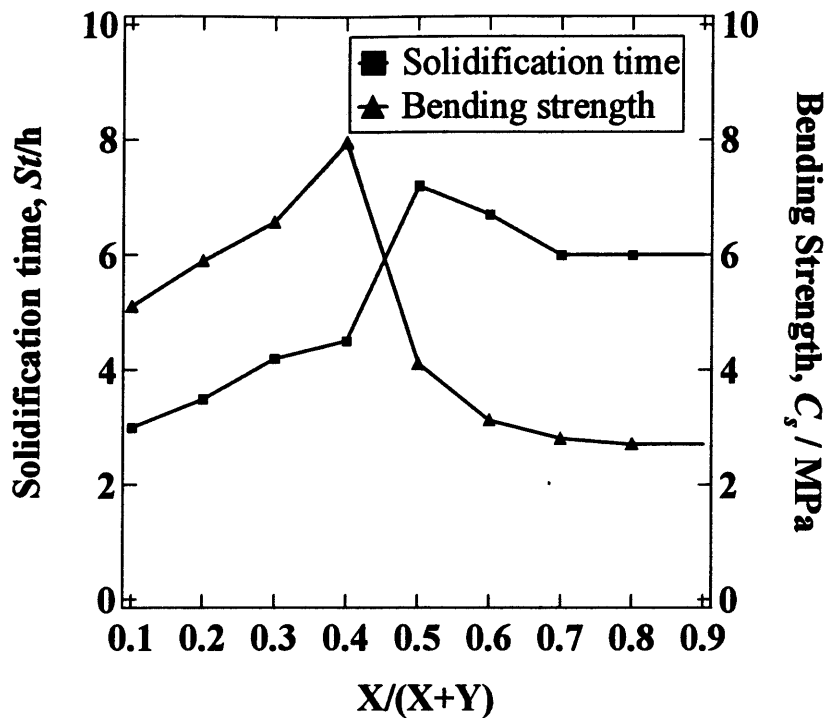
Figure 3.6 Relationship between solidification time and bending strength with different alumina-silica composites by mechano-chemical treatment (300 rpm and 60 min)

3.4 Conclusion

Ceramic green body of alumina-silica composites has been prepared with wide range of Al_2O_3-SiO_2 ratio by mechanochemically assisted chemical solidification. A milling process for obtaining activated ceramic powder having mechanochemically amorphized surfaces by milling ceramic powder. An alkali treatment process was obtaining a ceramic green body by adding alkali water solution. Mechano-chemical treatment of alumina-silica composites is found to promote Al-O-Si bonding between alumina and silica components. New bonding or new composition formed at a high silica content range. Mechano-chemical treatment could provide a useful technique for synthesis alumina-silica composites which can be obtained from cheap raw materials.

Reference

[1] B. D. Stojanovic, Mechanochemical synthesis of ceramic powders with perovskite structure. J. Mater. Pro. Tech., 143-144 (2003) 78-81.

[2] C. Damm, M. R. Mallembakam, W. Peukert, Effect of grinding conditions on mechanochemical grafting of poly (1-vinyl-2-pyrrolidone) onto quartz particles. Adv. Pow. Tech., 21 (2010) 50-56.

[3] M. Takahashi, M. Oya, M. Fuji, Transparent observation of particle dispersion in alumina slurry using in situ solidification. Adv. Pow. Tech., 15 (2004) 97-107.

[4] S. Blonski, S. Garofalini, Molecular dynamics study of silica-alumina interfaces. J. Phys. Chem., 100 (1996) 2201-2205.

[5] R. A. Fletcher, K. J. D. MacKenzie, C. L. Nicholson, S. Shimada, The composition range of aluminosilicate geopolymers. J. Eur. Ceram. Soc., 25 (2005) 1471-1477.

[6] D. S. Perera, J. D. Cashion, M. G. Blackford, Z. Zhang, E. R. Vance, Fe speciation ingeopolymers with Si/Al molar of ~2.

[7] K. J. D. MacKenzie, D. R. M. Brew, R. A. Fletcher, R. Vagana, Formation of aluminosilicate geopolymer from 1:1 layer-lattice minerals pre-treated by various methods : a comparative study. J. Mater. Sci., 42 (2007) 4667-4674.

[8] D. Oleszak, A. Grabias, L. Karwacinski, T. Kulik, Phase transformations in M2 steel powders subjected to ball milling. Rev. Adv. Mater. Sci., 8 (2004) 138-142.

[9] H. Su, J. Zhang, C. Cui, L. Lui, H. Fu, Rapid solidification bahaviour of $Al_2O_3/Y_2Al_5O_{12}$ (YAG) binary eutectic ceramic in situ composites. Mater. Sci. Eng A. 479 (2008) 380-388.

[10] I. Ganesh, N. Thiyagarajan, D. C. Jana, P. Barick, G. Sundararajan, J. M. F. Ferreira, Dense β-SiAlONs consolidated by modified hydrolysis-assisted solidification route. J. Eur. Ceram. Soc., 28 (2008) 879-885.

[11] J. Temuujin, K. Okada, K. J. D. MacKenzie, Effect of mechanochemical treatment on the crystallization behaviour of diphasic mullite gel. Ceram. Inter., 25 (1999) 85-90.

[12] J. Temuujin, K. Okada, K. J. D. MacKenzie, Formation of mullite from mechanochemically activated oxides and hydroxides. J. Eur. Ceram. Soc., 18 (1998) 831-835.

[13] M. Yasuoka, K. Okada, T. Hayashi, N. Otsuku, Property changes of mechanochemically treated alumina powder by annealing. Ceram. Inter., 18 (1992) 131-135.

IV. FABRICATION OF NON FIRING CERAMICS BY MECHANO-CHEMICAL TREATMENT USING PLANETARY BALL MILL

4.1 Introduction

In Chapter 3, with the development of mechano-chemical treatment, several compositions of alumina-silica composites ratio have been studied and successfully established the fabrication alumina-silica composites assisted mechano-chemical treatment. In this Chapter, fabrication of non firing ceramics from waste material has been successfully by mechano-chemical treatment using planetary ball mill. Paper sludge ash was used as starting material because in recent years, sludge from paper industry has been one of the serious problems concerning environment. The paper sludge were usually landfilled or burned to produce ash (paper sludge ash, PSA) that has been annually increasing in industrial countries. Lately, research work involving PSA was used as an additive raw material for cement industry. But, only small amount of PSA could be used as an additive to cement manufacturing process [1-2] and as a possible material for artificial aggregates [3]. The rest were mostly disposed by dumping, that could rise to serious environmental pollution (ex.; water pollution). Hence, developing a technique to utilized PSA could be significantly essential as a research study for investigating recycle waste materials. In the previous studied, it has been reported that PSA was composed of several oxides namely alumina, silica and calcium [3-4]. This inorganic oxide's materials had been the basic component for manufacturing ceramic materials that could be utilized as an initial material for ceramic products if properly investigated.

In this study, the effects of the operational conditions in the MC treatment process such as rotational speed and milling time on the mechanical properties of the solidified body were

investigated to fabricate non-firing ceramic products.

4.2. Experimental Procedure

The sludge ash powder from the paper industry was used as a raw material. Planetary ball mill was used for MC treatment under air at room temperature. In case of rotation speed and milling time conditions, each milling was carried out with a 100 g sample in a 500 ml capacity ceramic zirconia pot with zirconia balls of 10 mm in diameter. The mill was rotated at different speed interval up to 300 rpm at 60 min and with different time interval up to 60 min at 300 rpm.. Then treated powder was mixed with 3 mol dm^{-3} of KOH at 2,000 rpm for 5 min with an electric mixer. After the mixing, the slurry was poured into the Teflon mold and kept at room temperature until it becomes solid, ready for demolding. Then the specimens were dried at 25°C (RH 90%) for 7 days in the steam oven.

4.3 Results and Discussion

Figure 4.1 shows that the XRD patterns of the raw material and MC treated materials at different rotational speed and milling time. As shown in the graph, the raw material and MC treated materials were mainly composed of gehlenite ($Ca_2Al_2SiO_7$), Calcium disilicate ($CaSi_2O_5$), Dicalcium silicide (Ca_2Si) and Calcium aluminium silicide ($CaAlSi$). Intensity peaks of crystalline PSA materials were broad, smooth with decreasing intensity as the rotation speeds, milling time and diameter of ball increased. This indicates that the particles were in the state of miniaturization and amorphilization which is due to the influence of high energy action of planetary ball mill. In this case, the effectiveness of surface activation of PSA by mechano-chemical process can be done. On the other hand, the peak intensity of the solid specimen in figure 4.2 shows a significant increase of calcium disilicate minerals near (2θ) 30°, if compared

with figure 4.1 (treated powder). It is clearly shown that the occurring calcium disilicate peaks was directly proportional to alkaline reaction (K^+) as an effect on chemical reaction, attributable to the forming of Si-O bond from -SiO⁻M⁺ (M=K) group, or Si-O-Al bond within a highly Al and Si-substituted PSA structure (consistent with the assumption that the Al-rich and Si-rich of PSA leaching from mechano-chemical activation should be an efficient reacted with alkaline solution and forming to new chemical bonding [5-6]. At the same time, intensity peaks of crystalline in figure 4.2 were decreased with increasing the rotation speed and milling time as previous mentioned.
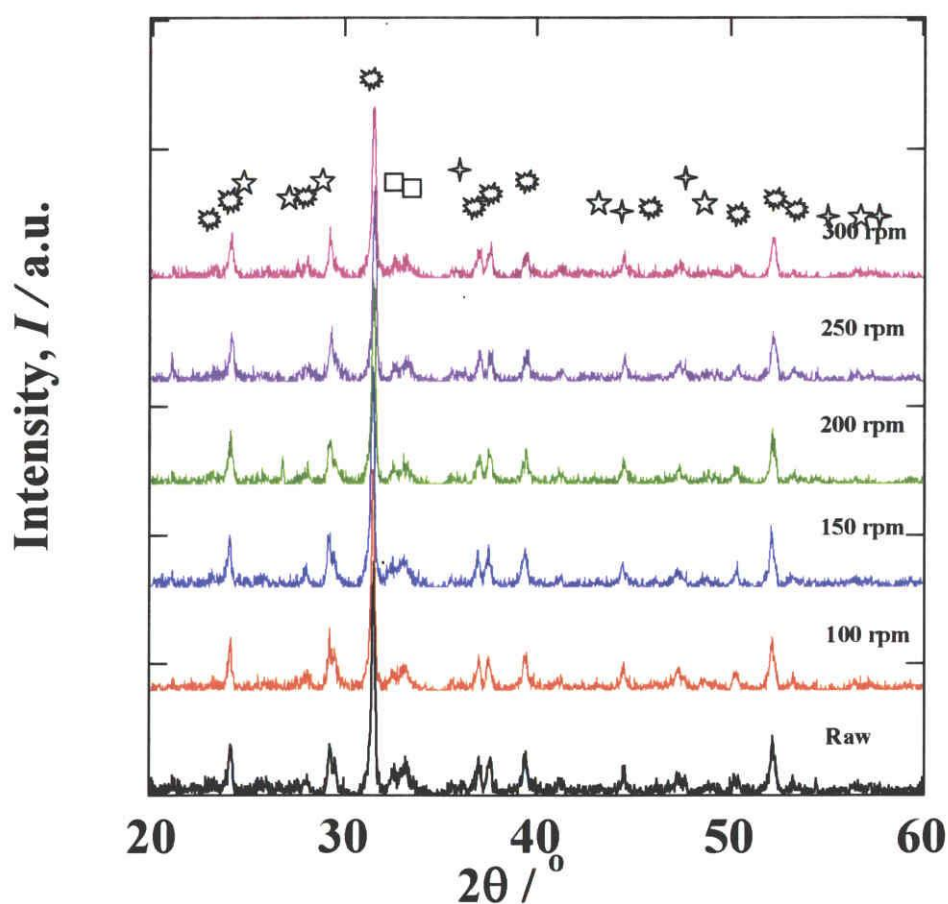
(a)
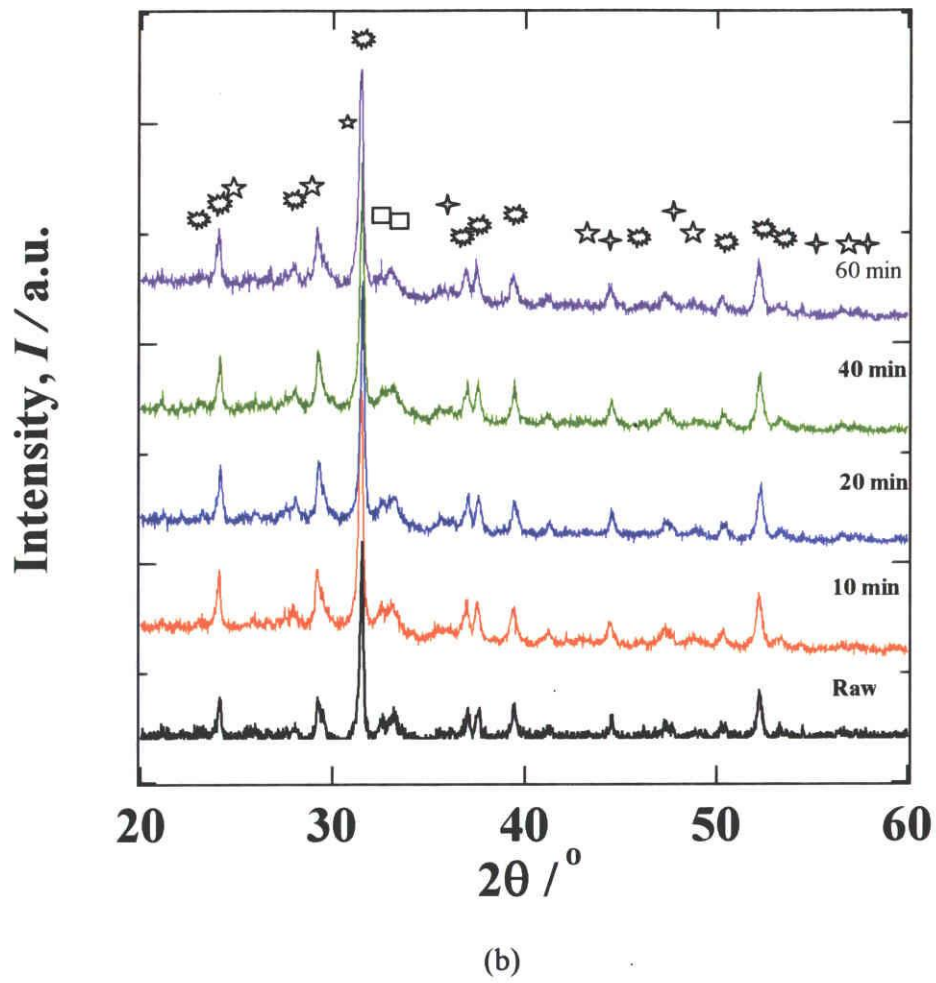
Figure 4.1. XRD patterns of mechano-chemical treated material by planetary ball mill;

(a) different rotation speed, (b) different milling time

(a)
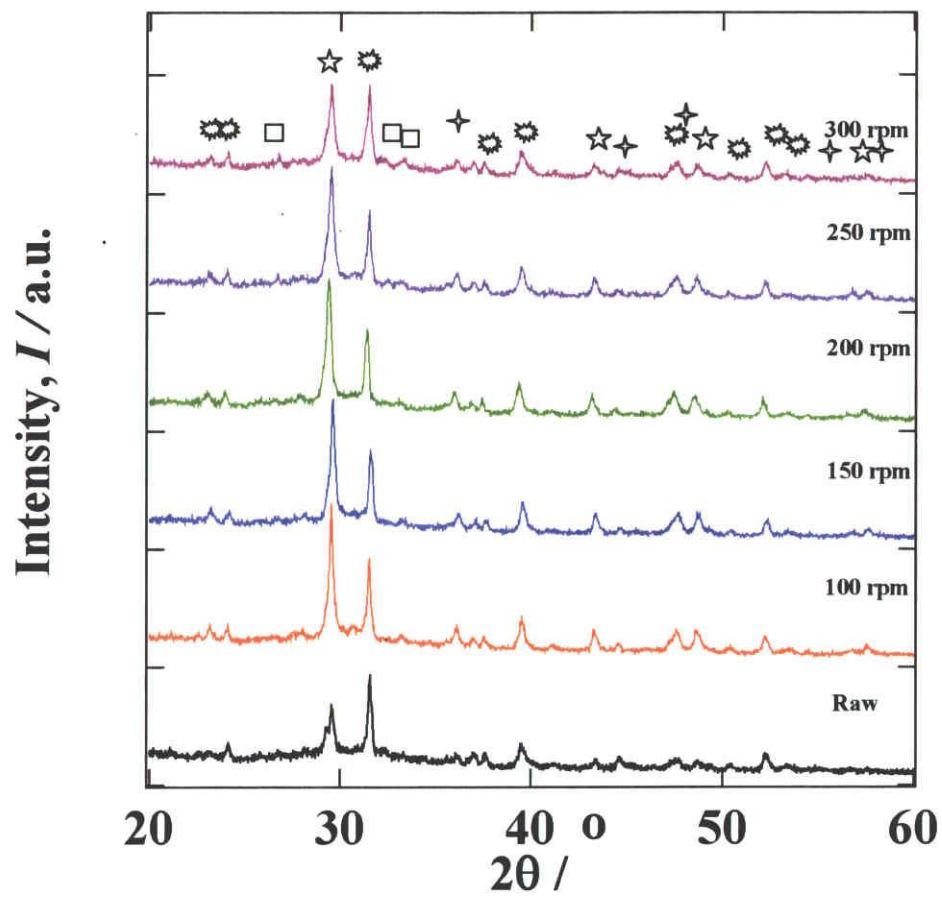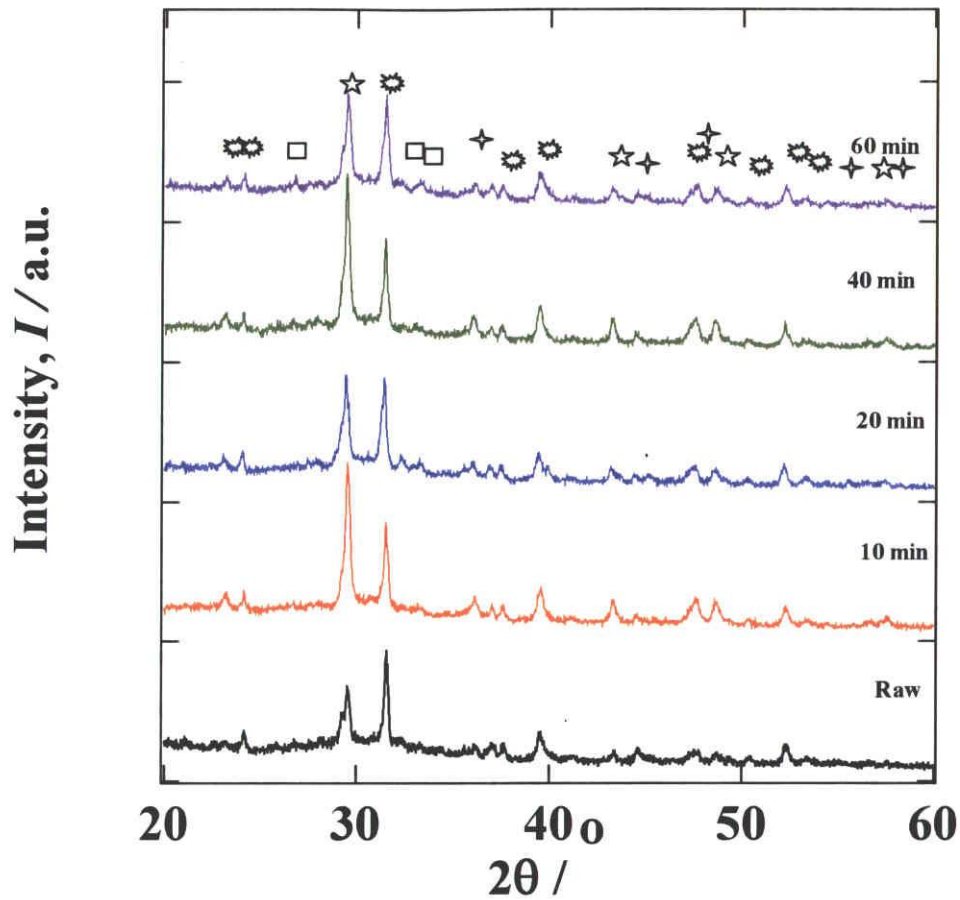
Figure 4.2. XRD patterns of solidified green body;

(a) different rotation speed, (b) different milling time

(✿ ($Ca_2Al_2SiO_7$), ★ ($CaSi_2O_5$), ✦ (Ca_2Si), ▫ (CaAlSi))

In figure 4.3 shows the relationship between the mean particle size of samples with MC treatment under various conditions. As shown, the rotation speed, milling time and diameter of ball of MC treatment had a great effect on particle size of the raw material. As observed, the particle size decrease at a certain point when the rotational speed and milling time were varied which coincide with the SEM analysis in figure 4.5. The results showed that average mean particle size (d_{50}) was

approximately between 4 to 28 μm after the samples subjected to planetary ball mill as compared to the raw powder. But at higher rotational speed and increasing the milling time, (longer than 150 rpm and 10 min, respectively), the mean particle size were almost the same. Then after 250 rpm of rotational speed and after 40 min of milling time the particle size tends to increased. In this manner, the reduction of particle size can decrease the distance between vacancy sites and enhance the vacancy diffusion to external surface and help formed new phase and grain growth. There were some reasons for this one is that the particle size of PSA only changes a little when the rotation speed increase from 150 to 300 rpm and the milling time increases from 10 to 60 min respectively. The other could be due to the very fine particle size that may have a small negative effect on milling because of agglomeration of fine particles.
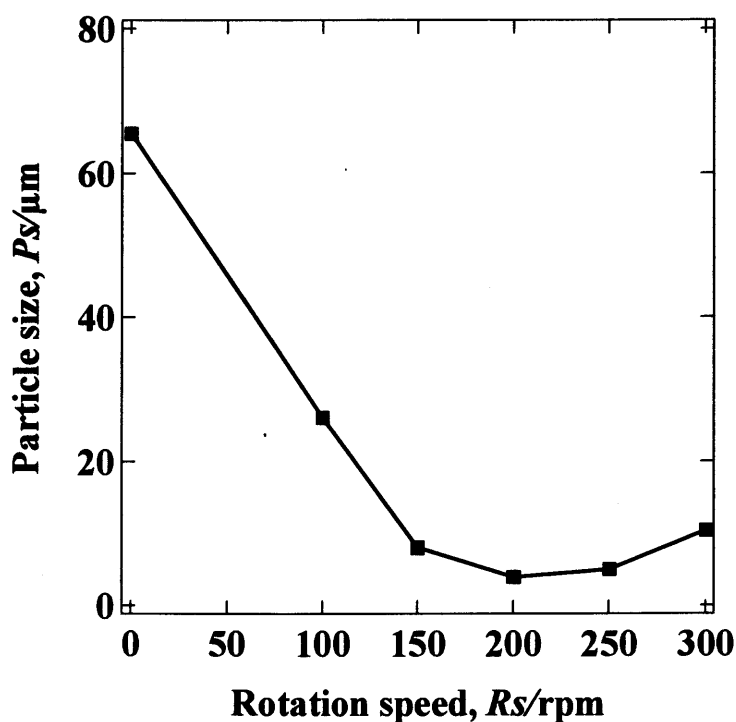
(a)
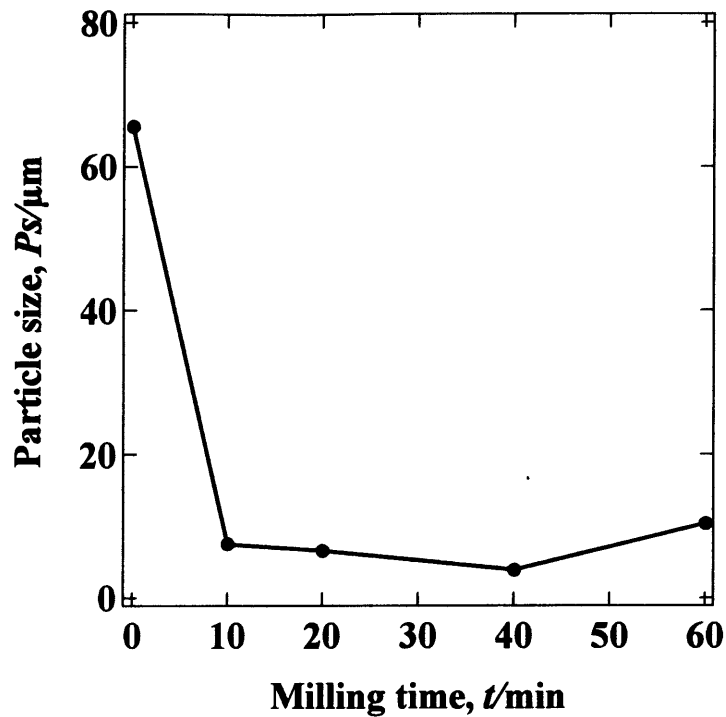
(b)

Figure 4.3. Mean particle size (d_{50}) distribution of mechano-chemical treated material by planetary ball mill; (a) different rotation speed, (b) different milling time

In figure 4.4 shows the specific surface area (BET) of samples with MC treatment at different condition such as the rotational speed and milling time. Based from the obtained results, the BET increased with increasing the rotational speed and milling time. Wherein the BET increased to a maximum value is 7.18 m^2g^{-1} during the 200 rpm of rotational speed, 9.04 m^2g^{-1} and during the 20 min of milling time, respectively. As observed, a larger surface area (BET) can be obtained during the milling of PSA using the planetary ball mill. But further milling the surface area (BET) of the sample decrease to about 5.95 m^2g^{-1} after 300 rpm of rotation speed and 60 min of milling time. This is a typical specific surface area change during mechano-chemical treatment. The increase in the BET during the first period of milling simply is a result of particle fracturing

induced by ball impacts and the later reduction in BET surface area is linked to the agglomeration effects at high energy. It should be noted also that adsorption on surface of particle was found in mechano-chemical treatment. These surface area (BET) results coincide again with the results of the particles size, SEM analysis and XRD analysis that there was indeed a change in surface particles of a treated PSA.

(a)
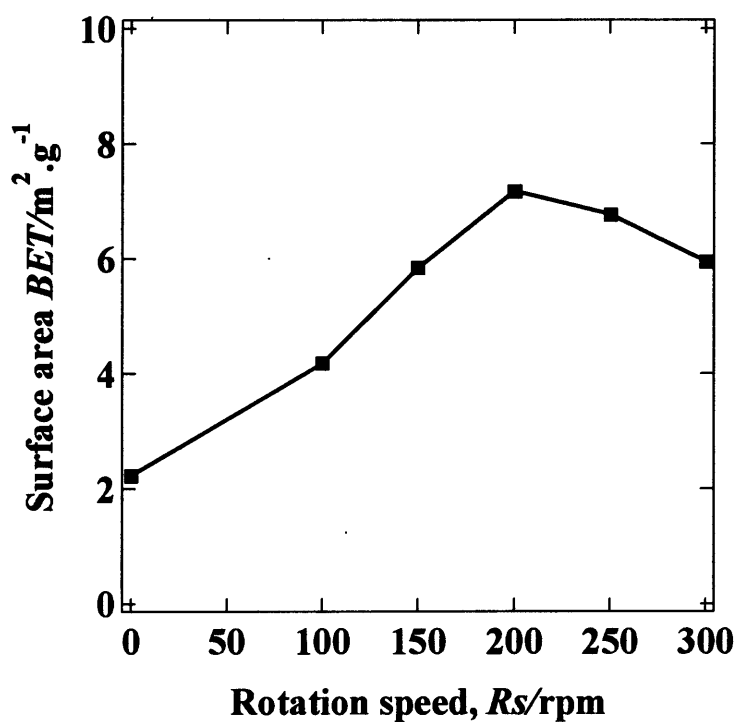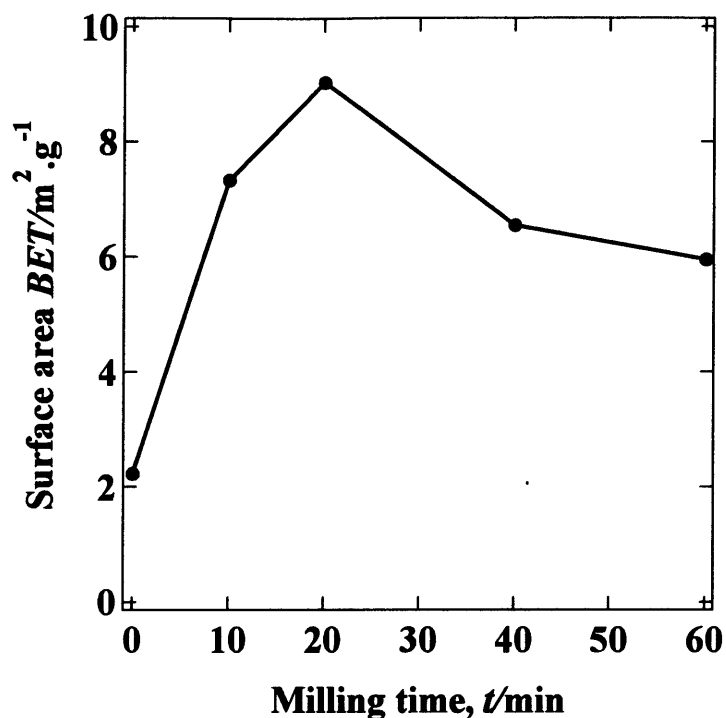
Figure 4.4. BET surface area of mechano-chemical treated material by planetary ball mill;

(a) different rotation speed, (b) different milling time

In this part, the microstructures of the samples were examined to investigate the developments of the MC treatment influences the raw material structure. The characteristic surface microstructures of raw material without and with MC treatment at different rotation speeds, milling time and diameter of ball using planetary ball mill were shown in figure 4.5, respectively. Figure 4.5(a) shows a scanning electron micrograph of raw PSA and treated PSA with different rotational speed and the figure 4.5(b) shows a scanning electron micrograph of treated PSA with different milling time. Based on the observed micrograph, the changes of micro-surface structure were achieved using the planetary ball mill with increasing rotation speed and milling time. The morphologies shows that the particle size of MC treated sample also decrease at a certain change

of rotational speed and milling time by planetary ball mill. But one should be cautious on increasing the rotational speed and the milling time because the small particles (MC treated) tend to agglomerate to form larger particles at high energy during higher rotational speed and longer milling time.

100-60

150-60

300-60

1 µm

(a)

300-10

300-20

300-40

1 μm
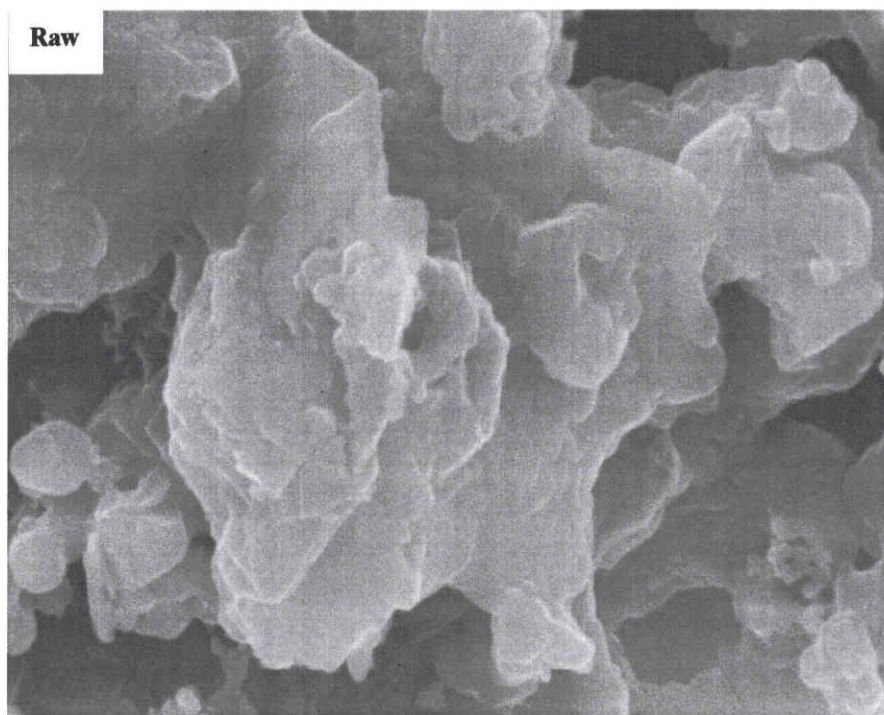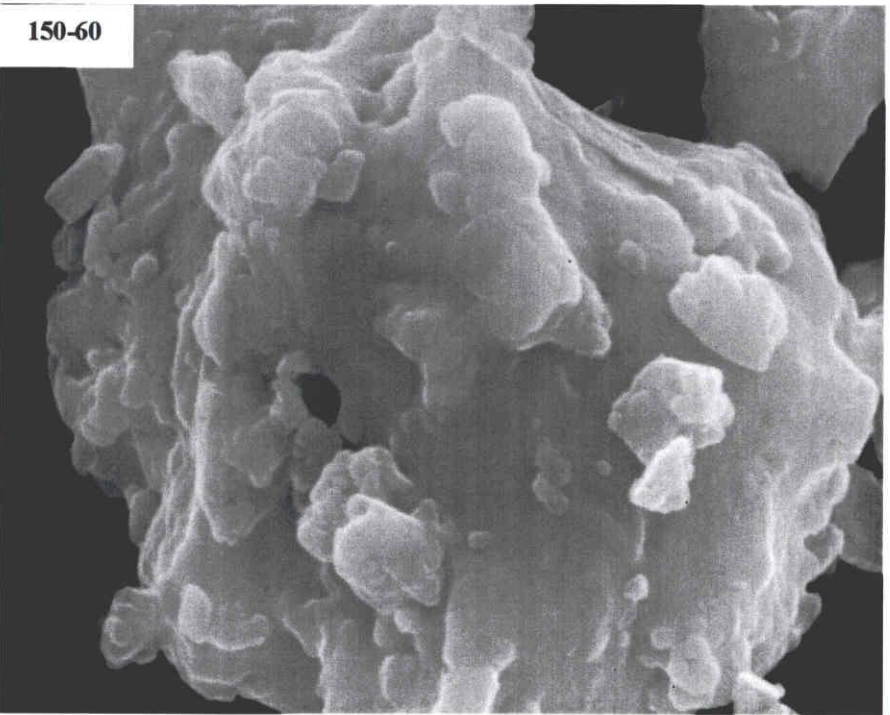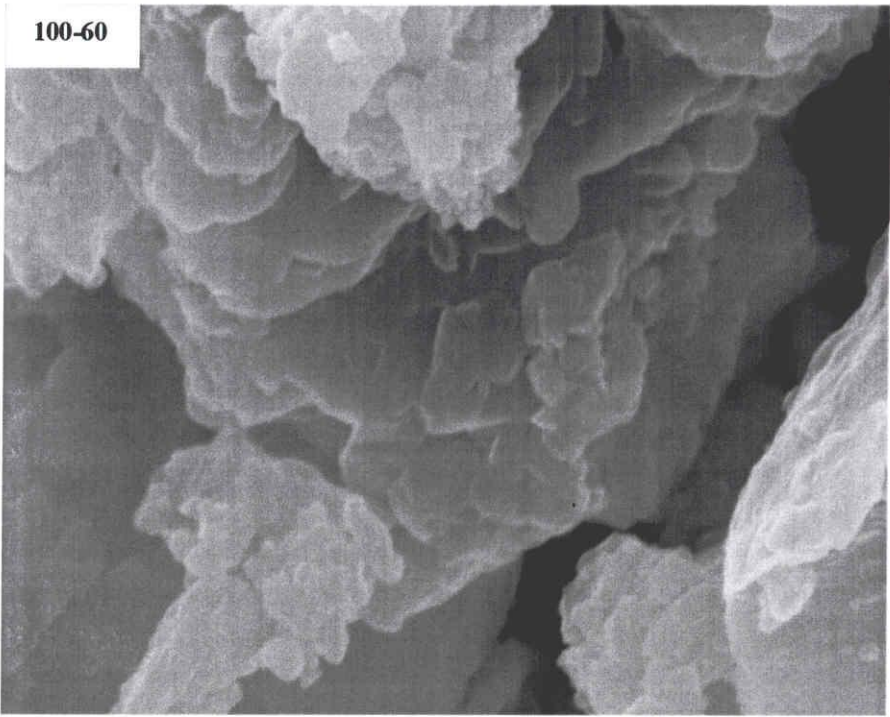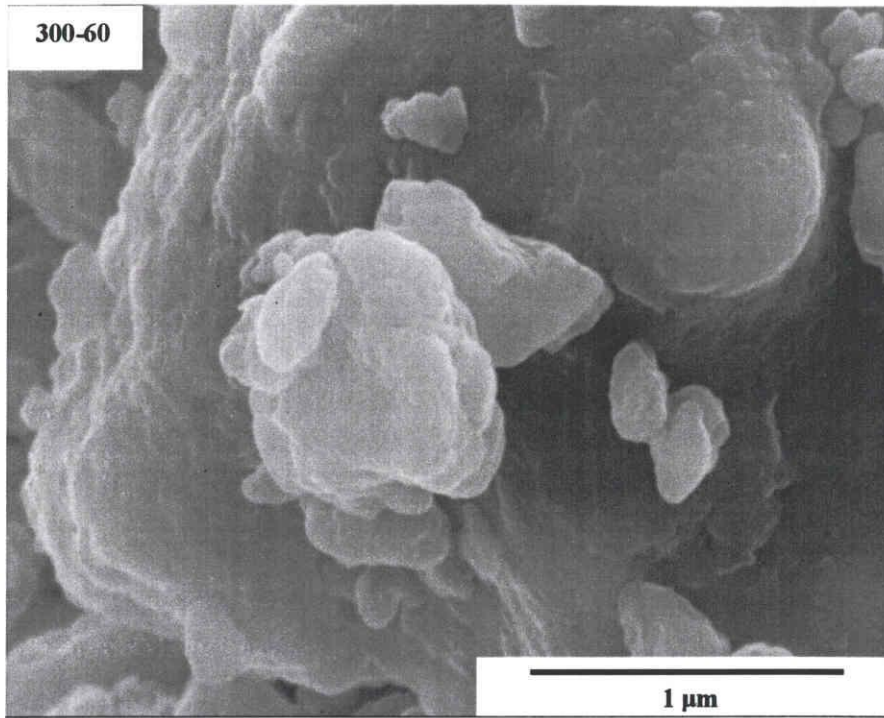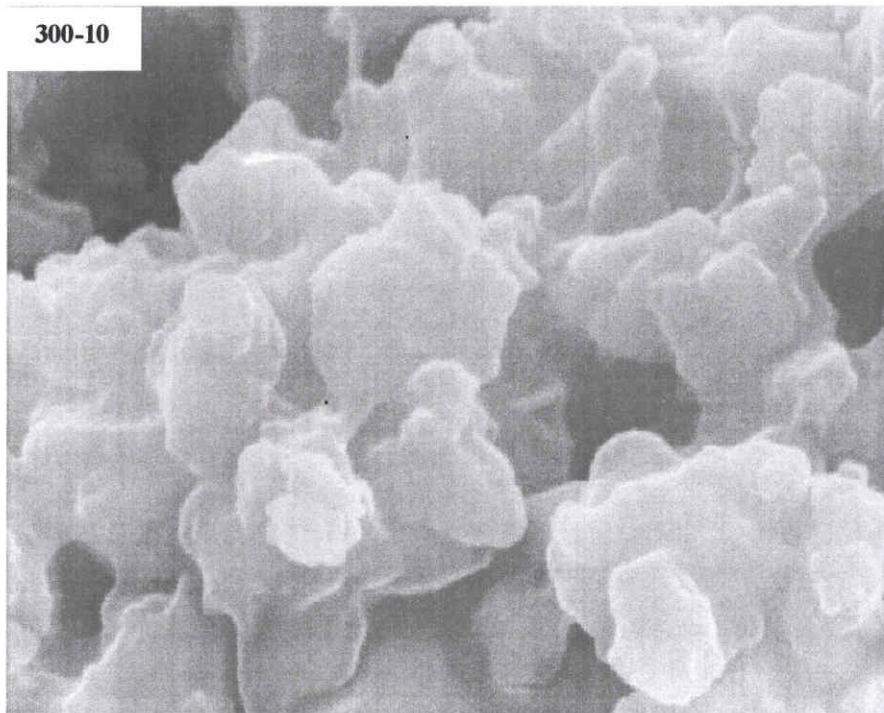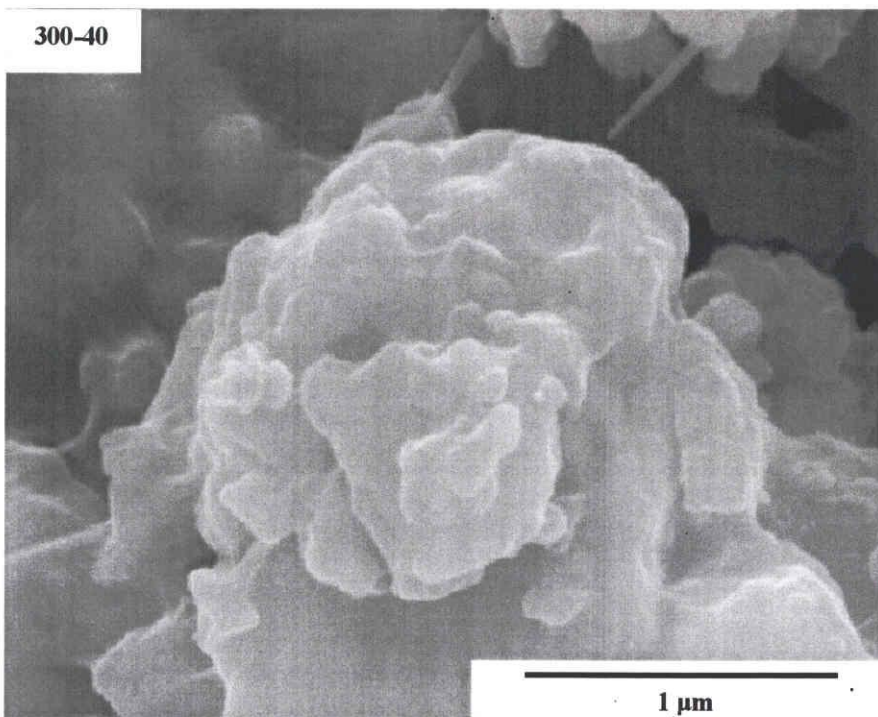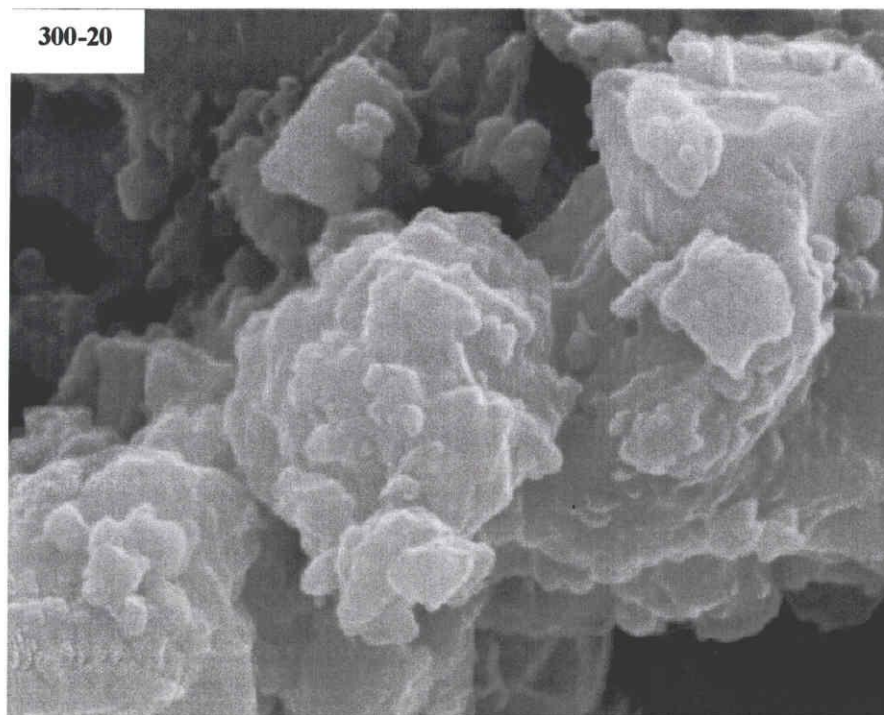
(b)

Figure 4.5 Microstructure of mechano-chemical treated material by planetary ball mill;

(a) different rotation speed, (b) different milling time

To observe the mechanical strength of the experimental sample, compression strength was investigated. In figure 4.6 shows the compression strength of specimens prepared by different MC treatment conditions. It can be observed that the compression strength of MC-treated specimen was clearly stronger than that of non-MC-treated specimen. These specimens showed that the compression strength was significantly increasing with effect of MC treatment. In general as observed in the obtained results, the strength of the specimens depends on the total number bonds between the interfaced surfaces of materials with MC treatment. In this case, it is tentatively considered that the MC treatment enhances surface activation and chemical reaction between the interfaced surfaces resulting in product layer bonding between adjacent particles. But, in the cases of high rotation speed as above 200 rpm and long milling time, the compression strength was decreased. It was considered that high energy milling leads to powder agglomeration or the density distribution of green body that contributed to reduction of mechanical properties. From results, one can analyzed that the MC treatment could be a powerful technique to obtained activated surface of powder. Advantage of proposed fabrication method is mechano-chemical treatment strongly affects on solidification and mechanical properties of solidified body.
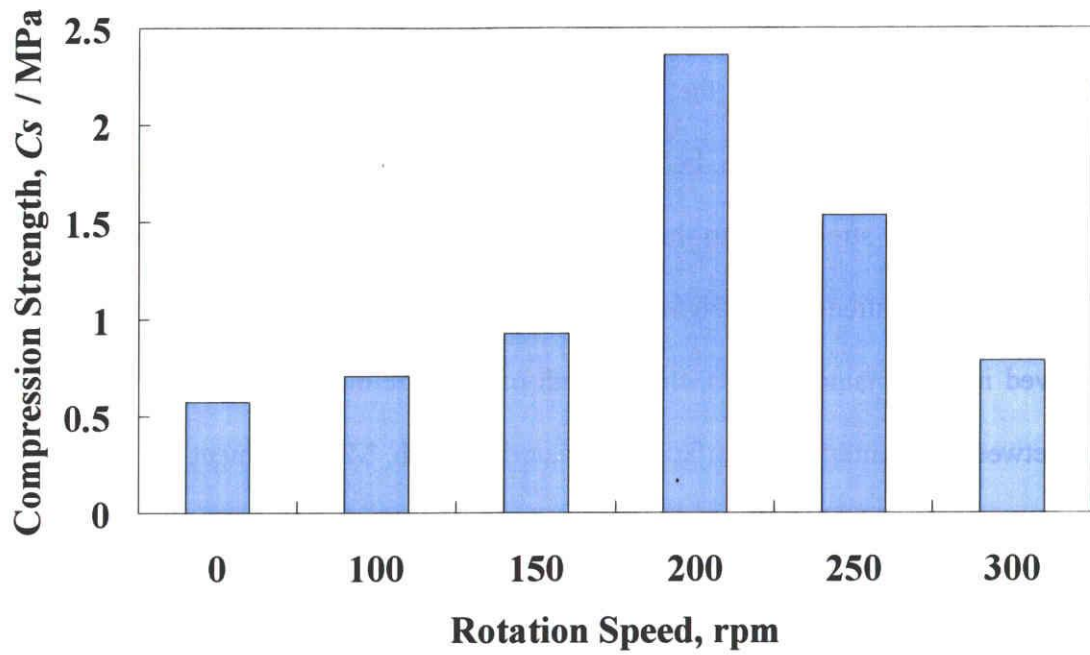
(a)
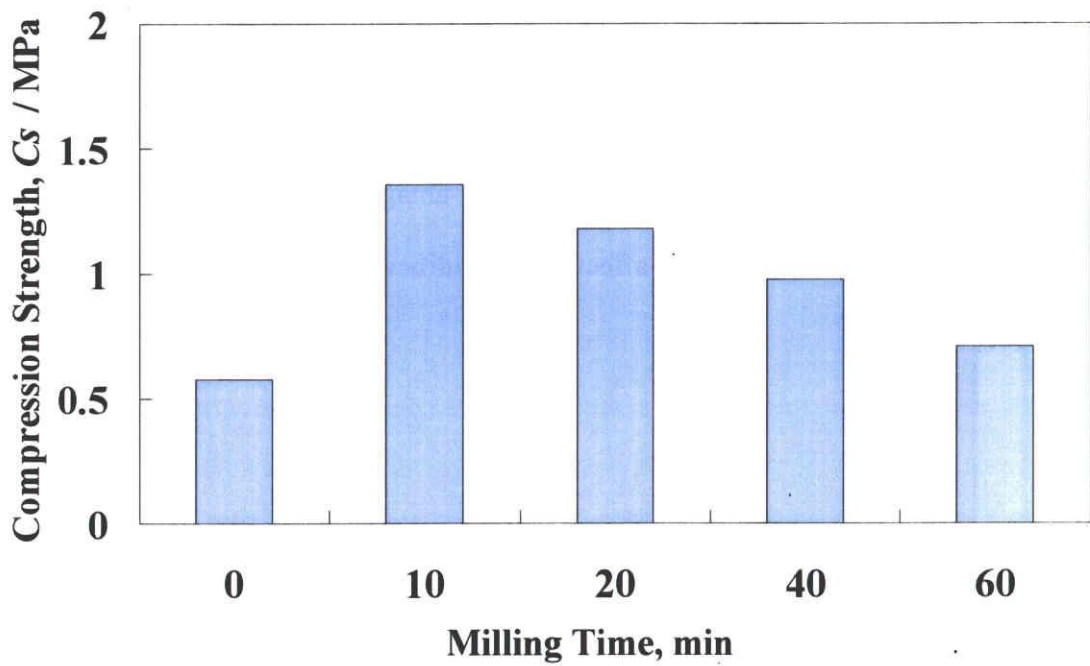
(b)

Figure 4.6. Compression strength of solidified specimens;

(a) different rotation speed, (b) different milling time

4.4 Conclusion

Non-firing ceramic from paper sludge ash was successfully fabricated by mechano-chemical with alkaline-chemical reaction process. The mechano-chemical treatment of planetary ball mill affects the fabrication of non-firing ceramics when the rotational speed and milling time were varied. The alkaline solution was used as a binder between ceramic particles forming a strong green body of specimen at room temperature. The chemical reaction depends on several factors such as the particle size distribution and mineral composition of paper sludge ash, kinds and concentration of the activator, reaction time, reaction temperature, etc. This process has an attractive route for shaping waste materials into valuable ceramics without firing process.

REFERENCES

[1] H. Eroglu, O. Ucuncu, H. H. Acar, The effect of sludge addition supplied from pulp mill on the compressive strength of cement, J. Uni. Chem. Tech. and Met., 42, 169-174 (2007).

[2] S. P. Mun, B. J. Ahn, Chemical conversion of paper sludge incineration ash into synthetic zeolite, J. Ind. Eng. Chem., 7, 292-298 (2001).

[3] Y. Kim, J.H. Kim, K.G. Lee, S.G. Kang, Recycling of dust wastes as lightweight aggregates, J. Ceram. Proc. Res., 6, 91-94 (2005).

[4] K. Okada, Y. Onoa, Y. Kameshima, A. Nakajima, K. J.D. MacKenzie, Simultaneous uptake of ammonium and phosphate ions by compounds prepared from paper sludge ash, J. Hazard. Mat., 141, 622-629 (2007).

[5] W.K.W. Lee, J.S.J. van Deventer, Chemical interactions between siliceous aggregates and low-Ca alkali-activated cements, Cem. Con Res., 37, 844-855 (2007).

[6] J. L. Provis, Modelling the formation of geopolymers; Doctoral Thesis, The University of Melbourne, 2006.

V. FABRICATION POROUS CERAMICS USING WASTE MATERIALS

BY NON-FIRING PROCESS

5.1 Introduction

In Chapter 4, the dense ceramics from white paper sludge ash (waste material from paper sludge industry) was successfully fabricated by mechano-chemical treatment. The idea from this study is attractive for fabrication porous ceramics. Porous materials have attracted interest because of the wide range of application such as filters, electronic sensors, catalysts and construction materials [1, 2]. There are various reports studies about the processing techniques in the fabrication of porous ceramics with properties, such as light-weight, high thermal stability, high chemical stability, and low thermal conductivity [3]. Firing ceramics is one of the most common techniques in fabrication porous materials. Basically, burning out of the material during sintering process [4, 5] and acid leaching [6] have been studied. However, this method has been disadvantageous in terms of high cost and can be harmful to the environment. In addition, some porous ceramics made by this method has a low strength and poor flexibility even if it has large surface area. Furthermore, in this conventional method, controlling the pore structure is limited [7, 8]. Fundamentally, porosity depends strongly on the morphology and particle size distribution. Hence, if the morphology and particles could be uniform, the pore structure can be uniformly distributed. Moreover in this process, aside from it can be easily controlled, it has a lower production cost compared to other existing methods [7-10].

This work is concerned with the fabrication porous ceramics from waste materials by mechano-chemical treatment. Black paper sludge ash (BPSA, waste materials) from sludge of paper industry is used as a starting material because it is waste product, Utilizing these waste materials

144

will help decipher some environmental problems like global warming (problems of excessive emission of CO_2 from human and industrial). The black paper sludge is a waste material (mixture of paper sludge, waste tire, waste oil and waste plastic) of pulp and paper industry which produced excessive CO_2 emission to the environment. Recycling these combustible waste materials can help reducing energy consumption and reduction of CO_2 emission wherein the quantity of waste paper sludge is drastically increasing. Moreover, waste from oil from turbine, tire, and plastic are also serious environmental issues because the amount of sludge waste disposed into the landfill increase. This practice is unacceptable because of the rapid depletion of available landfill site. Some industries burned the sludge wastes and produce BPSA [11-14].

This present study is focusing on the development of pore structure of BPSA by mechano-chemical effect and addition of alkaline solution at various reaction temperatures to fabricate porous ceramics material. Based on investigation in this chapter will divided 2 parts; First part will describe the effect of reaction temperature on the forming of porous structure of solidified porous ceramics in topic of Novel fabrication route for porous ceramics using waste material by non-firing process and second part will describe the effect of mechano-chemical treatment on the controllable porous structure of solidified porous ceramics in topic of Application of mechano-chemical process for fabrication of porous ceramics from waste materials.

5.1.1 Novel fabrication route for porous ceramics using waste material by non-firing process

5.1.2 Experimental Procedure

5.1.2.1 Sample preparation

BPSA received from S.K KOUSAN Co. Ltd., Japan used as raw material. The chemical compositions of received BPSA powder were shown such as SiO_2 30.0 wt%, Fe_2O_3 16.1 wt%,

CaO 14.3 wt%, Al_2O_3 11.3 wt%, ZnO 3.3 wt%, MgO 2.5 wt% and other 22.2 wt%. While the specific surface area (BET analysis) and mean particle size distribution of the BPSA powder (d_{50}) were 5.54 $m^2.g^{-1}$ and 14.41 µm respectively. The conditions for preparation of samples were followed. Planetary ball mill (Pulverisettle 5, Fritsch, Germany) was used for mechano-chemical process; set to 300 rpm in rotation speed and 60 minute in milling time under air at room temperature to obtain activated BPSA powder. Then, 10 g of received BPSA or activated BPSA powder was mixed with 10 ml of KOH solution at 5 $mol.dm^{-3}$, 5M (chemical synthesis). The slurry was poured into the mold after that it was kept at 25°C for received BPSA as raw and different reaction temperatures (25°C and 50°C) for activated BPSA as 5M-25°C and 5M-50°C in the oven respectively. After complete solidification of slurry, the solid samples were carefully taken out of the mold. Then, the solid samples were dried for 3 days in oven to obtain porous ceramics. The fabrication routes of porous ceramics without firing process are shown in figure 5.1.
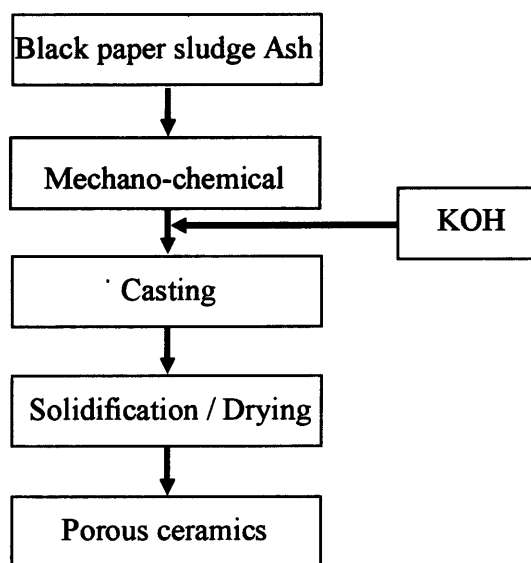
Figure 5.1 Fabrication route of porous ceramics without firing process

5.1.2.2 Characterization

Particle size distribution of powder was determined by particle size analyzer (MicroTrac MT3000II Series, Japan). The specific surface area of BPSA powder was determined with N_2 adsorption method at 77 K using an automatic gas adsorption-desorption apparatus (Belsorp-max, Japan). The composition and crystalline phase were observed by the X-ray diffraction, XRD (Model RINT 1000, Rigaku, Cu $K\alpha$, and 40kV). Surface structural and pore size observation were carried out using Micro Focus X-ray CT system (SMX-90CT, Shimadzu, Japan). The porosity and physical properties of solidified specimen were determined by mercury porosimeter (PASCAL Porosimeters, Thermo Electron S.p.A., Italy). The mechanical property was evaluated by diameter compression test using universal testing machine (Shimadzu AGS-G). All tests were performed at room temperature. The test results were recorded using an average value of three measurements.

5.1.3 Results and Discussion

5.1.3.1 Adsorption-desorption Properties of starting material

The adsorption-desorption isotherm of the received BPSA powder ash is shown in figure 5.2. The experiments were performed at 77 K, the boiling point of nitrogen at atmospheric pressure. N_2 sorption is the standard method for determining the pore size distribution of a porous material with pore size smaller than 100 nm. With this technique, the adsorbed amount of nitrogen is measured as a function of the equilibrium pressure in the gas phase. From the amount adsorbed nitrogen at a certain pressure, the pore volume can be calculated with a certain pore size present in the material. The N_2 isotherm of received BPSA powder can be classified into type II of IUPAC classification. Porous structure of received BPSA powder is mostly composed of non-

porous solids wherein the surface area as mentioned in sample preparation section (5.54 $m^2.g^{-1}$)

while pore size distribution showed the BPSA powder almost composed of macroporosity.
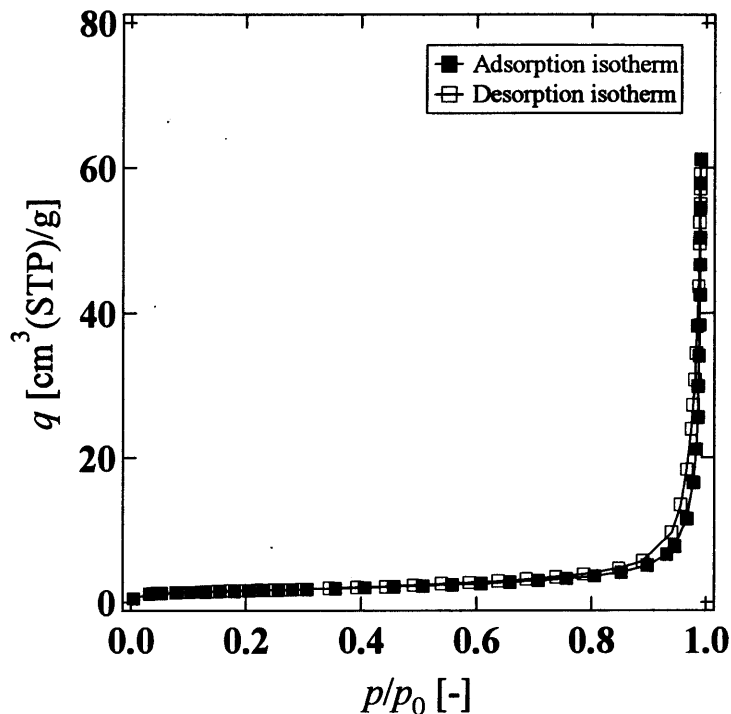
Figure 5.2 Adsorption and desorption isotherm of received BPSA powder

5.1.3.2 Properties of solidified non-firing bodies

Figure 5.3 shows the XRD patterns of solidified porous ceramics at different conditions of raw (non-activated powder), 5M-25°C and 5M-50°C (activated powder), respectively. The diffraction peaks and intensity of all the samples (crystalline BPSA) were sharp and similar. No changes in XRD patterns were observed. Based on the data gathered, Quartz (SiO_2), Hematite (Fe_2O_3), Anorthite ($CaAl_2Si_2O_8$), and Kyanite (Al_2SiO_5) are the major components found in the solid porous ceramics materials. Furthermore, after mechano-chemical treatment, the results slightly the formation of broaden peaks without new phases. This can be ascribed to small defects from the mechano-chemical treatment or glassy phase formation (amorphous state with shearing force).

On the other hand, the intensity peaks of crystalline BPSA were sharp and small peaks of kyanite are formed after chemical synthesis at high reaction temperature (5M-50°C) when compared with raw-BPSA (received BPSA powder) This is attributed to the formation of kyanite from minerals at high-pressure phase during chemical reaction [15-16].
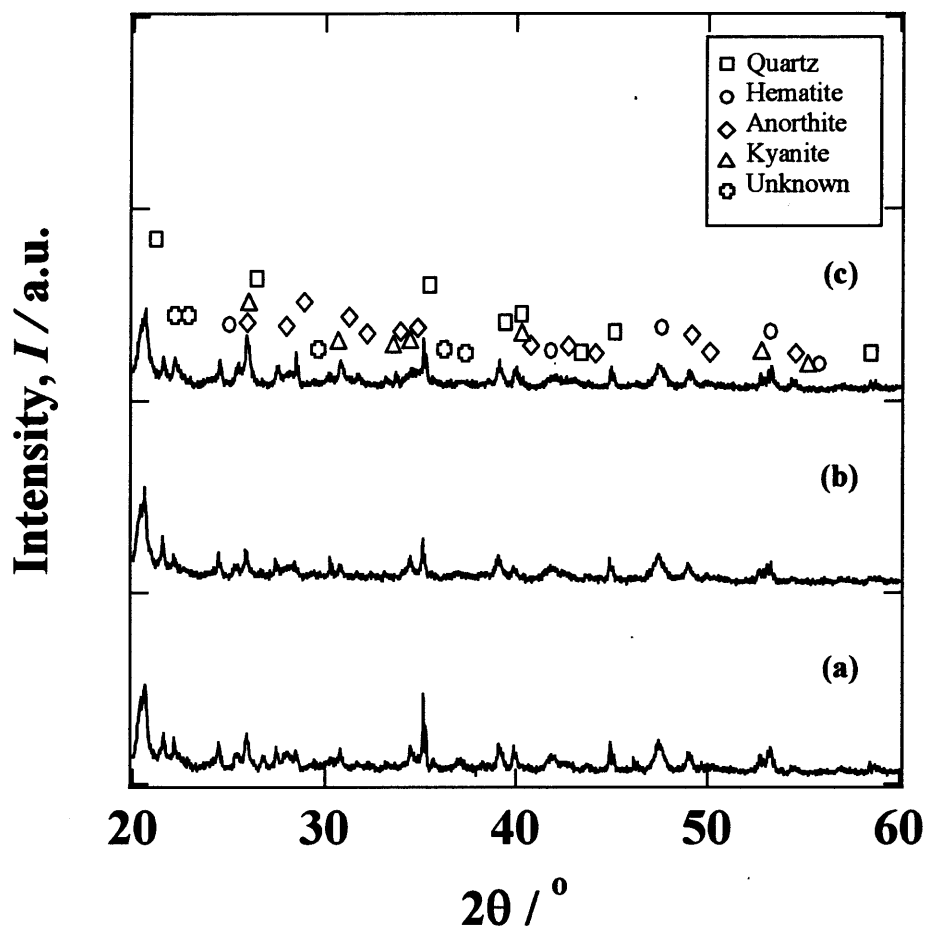
Figure 5.3 XRD patterns of solidified BPSA at different conditions

(a) raw, (b) 5M-25°C, (c) 5M-50°C

Table 5.1 Physical properties of solidified porous ceramics

Conditions of BPSA	Specific surface area [m^2/g]	Apparent density [g/cm^3]	Pore diameter [μm]	Total porosity [%]	Mecahnical strength [MPa]
raw	19.1	1.1	8.0	70	0.03
5M-25°C	25.4	1.8	0.3	45	0.53
5M-50°C	23.5	1.3	2.8	52	0.20

Figure 5.4 shows the non-firing porous ceramics with inset image of the cross section of raw-BPSA and activated BPSA at different reaction temperature. In case of raw-BPSA, figure (5.4a), a lot of holes were observed on the specimen leading to the fragile structure. Therefore, it was very difficult to handle with the fragilment of solidified raw specimen in order to characterize in more detail. On the other hand, the activated BPSA with alkaline solution as shown in figure (5.4b); 5M-25°C, and (5.4c); 5M-50°C, produced a solid of porous body with the chemical bonding effect from mechano-chemical process. It was revealed that the chemical bonding was occurred and then transformed to the new phase on the interfacial surface of powder after mechano-chemical activation [17]. With increasing the reaction temperature, the number of visible pore in solidified specimens was increased. There were a few visible pores in activated BPSA 5M-25°C as shown in figure (5.4b) due to the generation of gas (air bubbles) during the synthesis. These small pores assigned to the existence of air bubbles in the slurry, since air bubbles were not removed from slurry before solidification of the slurry. The mechanical strength

of solidified specimens of raw BPSA, 5M-25°C, and 5M-50°C is 0.03, 0.5,3 and 0.20 MPa, respectively as illustrated in table 5.1. From this result, the mechano-chemical treatment could be a powerful technique to obtained activated surface of powder. In the same way, the previous mention can be confirmed by the photograph of cross-section of solidified porous ceramics that simultaneously forms by gas generating from the composite materials. As raw material mixed with alkaline solution produced gas from chemical reaction and then solidified into a rod shape. From the inset in figure 5.4, the dark and grey colors correspond to pores diameter and green body, respectively. A visible pore size of specimen and number of pore increased with the raise of reaction temperature. It is broadly accepted that the reaction between particles is strongly promoted after collision. By increasing the reaction temperature, the mobility and collision rate of particles are concurrently promoted leading to the acceleration of the reaction rate. In this case, the pore size of synthesized ceramics is proportional to the reaction temperature during the forming of pore.

In addition, not only the reaction temperature but composition of waste material in BPSA also affects the formation of pores. The composition of waste material in BPSA leads to the generation of gas in slurry. This is a proposed novel method to fabricate porous ceramics.
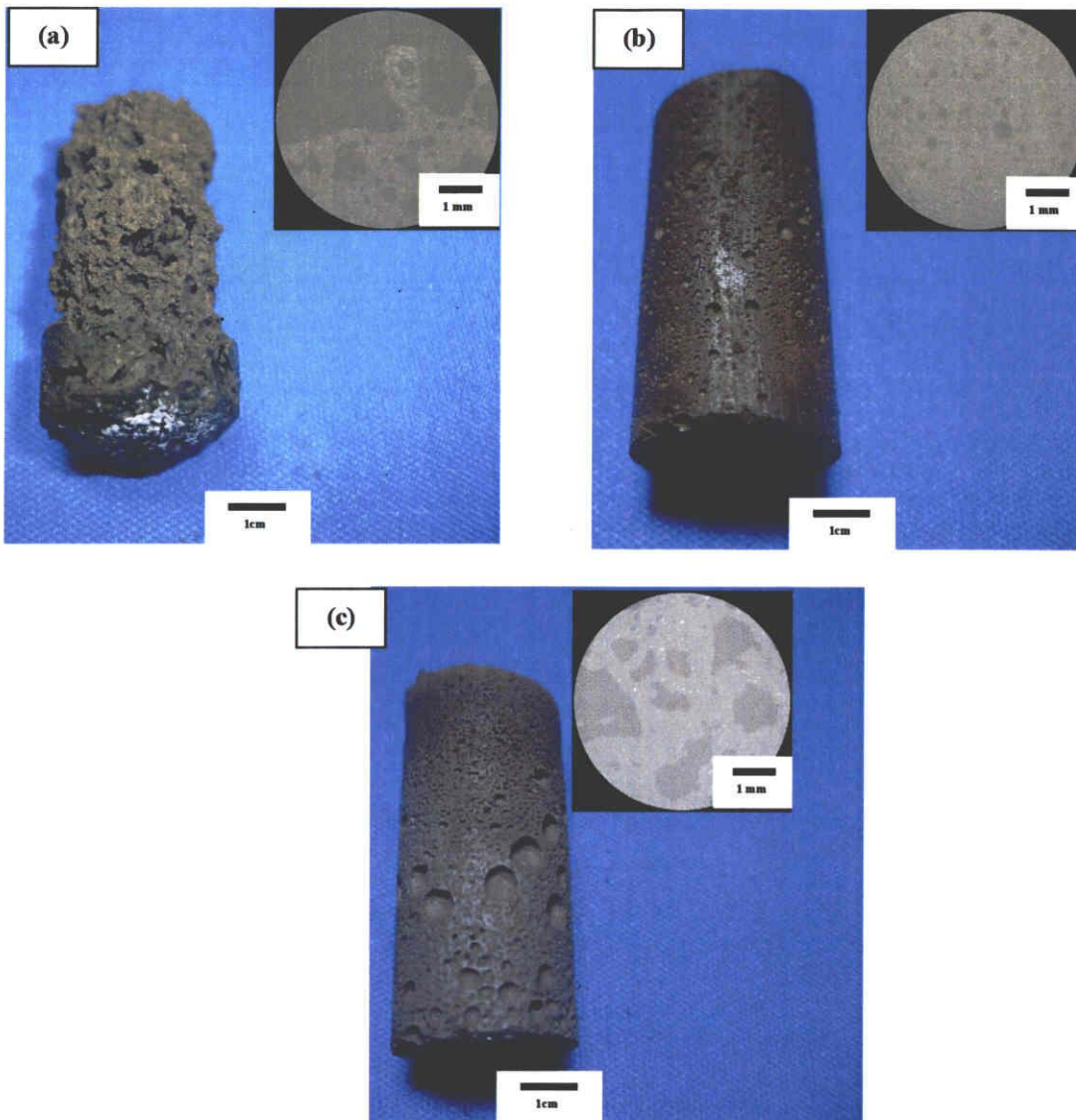
Figure 5.4 Non-firing porous ceramics and cross section fabricated from BPSA

(a) raw, (b) 5M-25°C, (c) 5M-50°C

Figure 5.5 shows pore size distribution and average pore size of solidified porous ceramics at different conditions. The average pore size of solidified porous ceramics of raw, 5M-25°C and 5M-50°C were 8.04, 0.32, and 2.75 μm, respectively. The pore size distribution graphs indicates the formation of macrospore (>0.05 μm). On the other hand, physical properties of the solidified porous ceramics were shown in Table 5.1. As the results, the porous properties have changed

with mechano-chemical process. With mechano-chemical process, the specific surface area, apparent density and mechanical strength increased, while pore diameter and total porosity decreased.
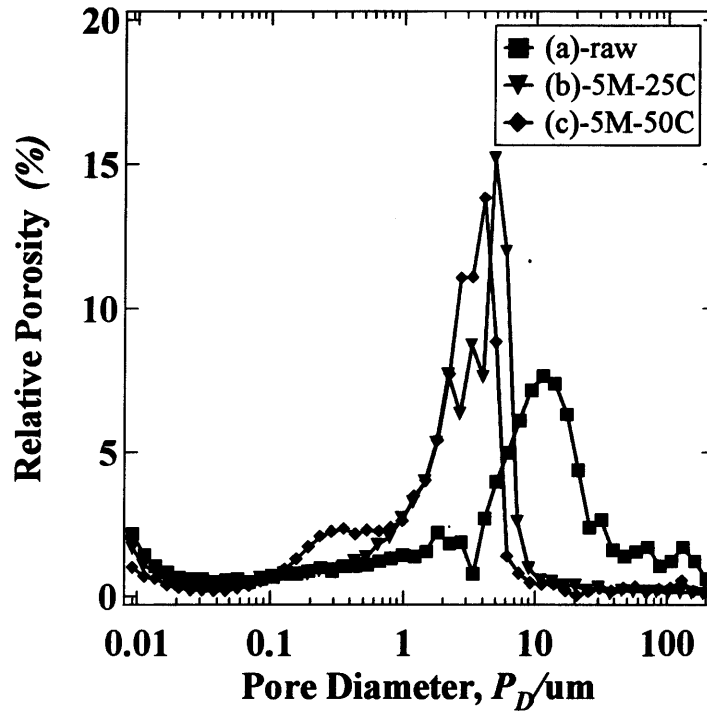
Figure 5.5 Relative porosity on pore size distribution of solidified porous ceramics

(a) raw, (b) 5M-25°C, (c) 5M-50°C

Hence, mechano-chemical treatment of solid material has been developed to produce new phases or compounds in solid state chemistry. It can affect the property of solid in two ways; destruction of the skeleton of the raw material to provide an amorphous phase and generation of various chemical processes to a new phase. On the other hand, the specific surface area, apparent density, mechanical strength, pore diameter and total porosity changed with the chemical reaction. The reaction temperature affected the increase of pore diameter, and total porosity, while specific surface area, apparent density, and mechanical strength were decreased.

Since porous structure was formed by the generation of gas during chemical reaction, which was assisted with the surface activation of the particles by mechano-chemical process. Macropores were generally observed in the specimens. The porous structures were generated during the reaction between alkaline and particle, resulting in the production of gas. The optimization of synthesis was at 5M-25°C condition because it provided the highest mechanical strength of solidified BPSA. The functions of porous ceramics are affected by not only pore size, but also pore structure and other attributes.

This research and development of these porous ceramics are attractive in various applications including filter, ultra light building materials, etc.

5.1.4 Conclusion

Porous ceramics were successfully fabricated from black paper sludge ash by non-firing process. The composition of tire and waste material in black paper sludge ash was studied. It was confirmed that the addition tire ash influenced the gas generating in slurry. The mechano-chemical treatment with alkaline activation was used as a chemical synthesis of ceramic particles to form porous structure of solidified specimen by gas generating. This fabrication technique has an attractive route for shaping waste material into valuable porous ceramics without conventional firing process. This research work demonstrated an easy method to control pore size of porous ceramics utilizing waste materials (BPSA).

Further experiments and research are recommended to explore the effect of other variables such as concentration of alkaline solution, kind of alkaline solution, and mechano-chemical conditions.

5.2.1 Application of mechano-chemical process for fabrication of porous ceramics from waste materials

5.2.2 Experimental procedure

5.2.2.1 Sample preparation

Planetary ball mill (Pulverisettle 5, Fritsch, Germany) was used for mechano-chemical activation under air at room temperature. The mill was rotated at 100-300 rpm in rotation speed at 60 min and 10-60 min in treatment time at 300 rpm. Then, the activated powder was mixed with 5 mol.dm^{-3} KOH solution and kept in mold at 25°C in steam oven 50% relative humidity until become solid ready for 3 days to obtain solidified porous ceramics (green ceramics body).

5.2.2.2 Characterization

The qualitative determination of the composition and crystalline phase present material were observed by the X-ray diffraction, XRD (Model RINT 1000, Rigaku, Cu Kα, and 40kV). The detection of trace metal in solution was carried out by ICP analysis (SPS-7800). Surface microstructural observation was carried out using a Field emission scanning electron microscopy, FE-SEM (JSM-7000F). Surface structural and pore size observation was carried out using Micro Focus X-ray CT system (SMX-90CT). The porosity and physical properties of solidified specimen was determined by mercury porosimeter (PASCAL Porosimeters, Thermo Electron S.p.A., Italy). The mechanical property was evaluated by diameter compression test using universal testing machine (Shimadzu AGS-G). All tests were performed at room temperature. The test results were recorded using an average value of three measurements.

5.2.3 Results and Discussion

The XRD patterns of the BPSA were treated at different mechano-chemical treatments in absence of additive is shown in Figure 5.6. As a result, no changes of XRD patterns were observed. Based on the XRD data, Quartz (SiO_2), Hematite (Fe_2O_3), Anorthite ($CaAl_2SiO_8$), and Kyanite (Al_2SiO_5) are the major components found in the starting materials. Furthermore, the intensity peaks slightly decrease and broadened with high rotation speed and prolong milling time. This can be indicate that the formation of amorphous phase with shearing force during mechano-chemical treatment. On the other hand, the relationship between particle size and BET surface area of powder produced though the mechano-chemical process is shown in Figure 5.7. With increasing of rotation speed and milling time, the particle size decrease but BET surface slightly increase. This is because of the size reduction during milling in planetary ball mill lead to the produced larger BET surface area. The planetary ball mill can be produced large surface area in particular in high rotation speed and prolong milling time probably due to stressing of particles in shear mode and generation of higher temperature.
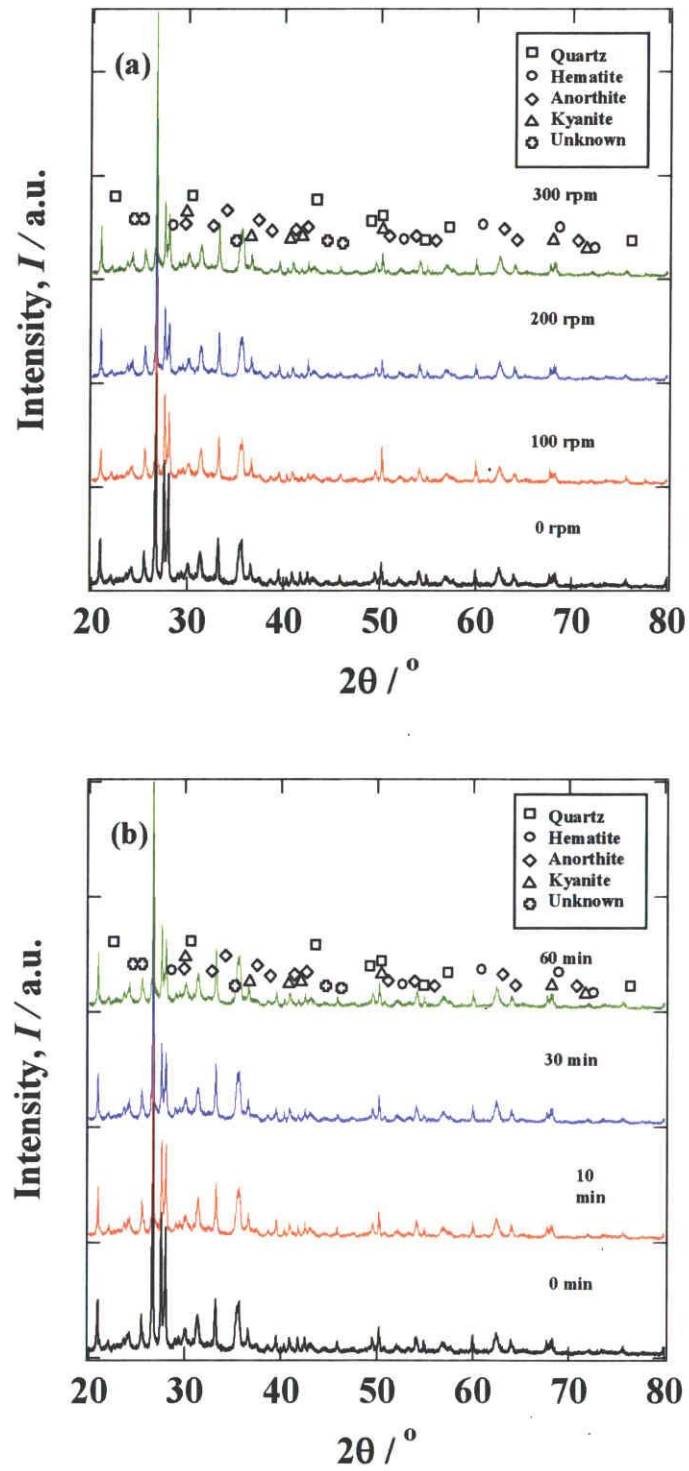
Figure 5.6 XRD patterns of activated BPSA at different mechano-chemical treatments;

(a) rotation speed, (b) milling time
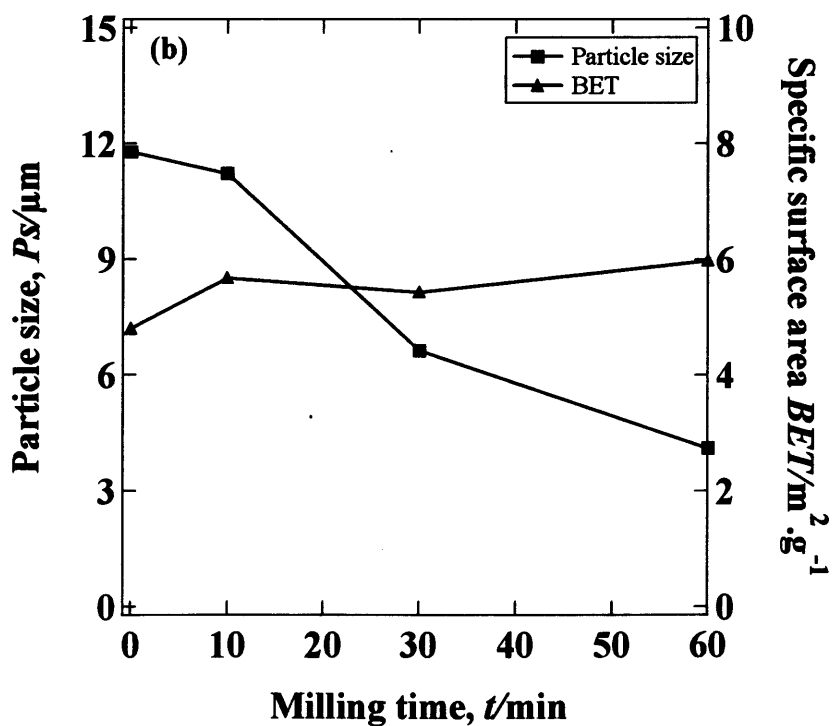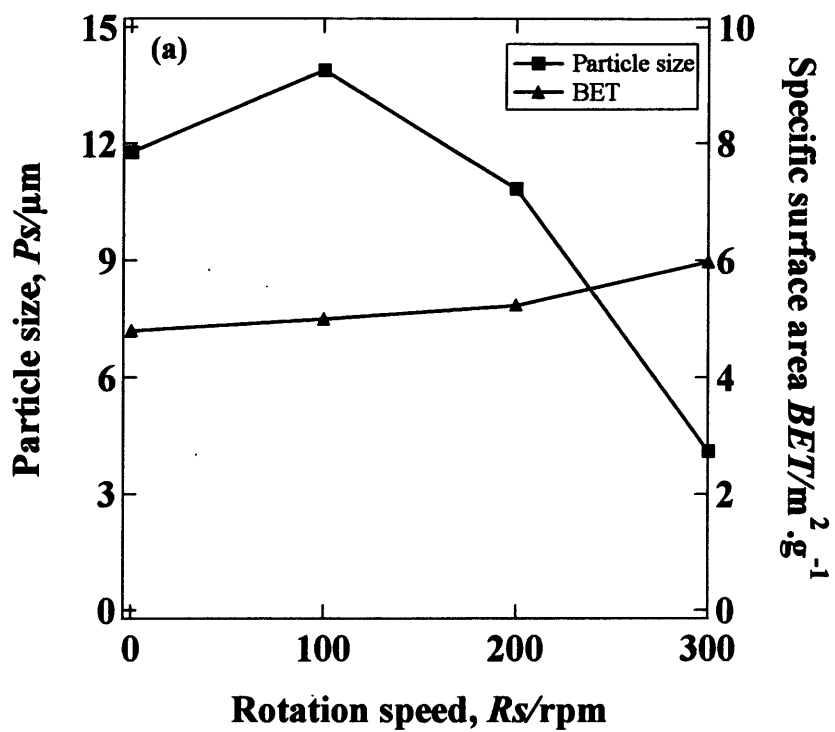
Figure 5.7 Relationships between mean particle size and BET surface area at different mechano-

chemical treatments; (a) rotation speed, (b) milling time

The presence of elements is composed in the BPSA. These elements gradually build up in the BPSA because of mechano-chemical treatment. For this reason, the analysis of BPSA is often referred to as wear metal or trend analysis. ICP technique can be used to accurately identify and predict component supply the necessary through put. For example, both Al and Si are usually present in the BPSA at the single ppm level. Figure 5.8 shows quantitative evolution of aluminum ion and silicon ion at different rotation speed and milling time. These results confirm the leaching of concentration of aluminum ion and silicon ion increases significantly with mechano-chemical treatment.

Figure 5.9 shows pore size distribution and average pore size of solidified porous ceramics at different mechano-chemical treatment. The pore size distribution graph indicates the formation of macropore (>0.05 μm). The average pore size of solidified porous ceramics of raw and mechano-chemical treated powder; 100-60, 200-60, 300-60, 300-10, and 300-30 were 2.20, 2.24, 1.90, 3.05, 1.76, and 2.05, respectively. With increasing the mechano-chemical treatment, the pore size distribution also increased.
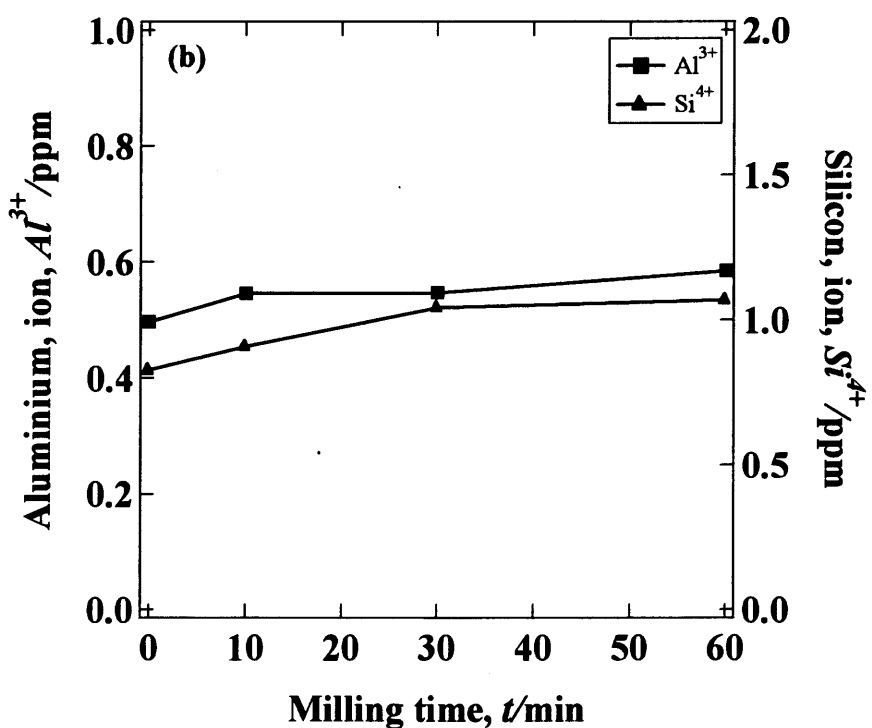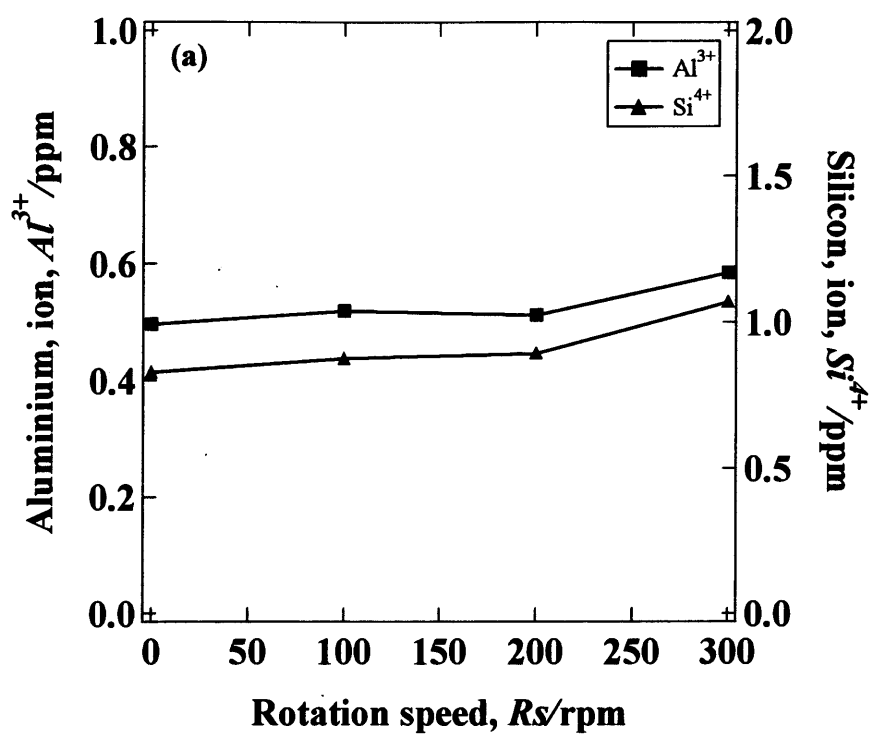
Figure 5.8 Elution behavior of aluminium and silicon ion at different mechano-chemical

treatments; (a) rotation speed, (b) milling time
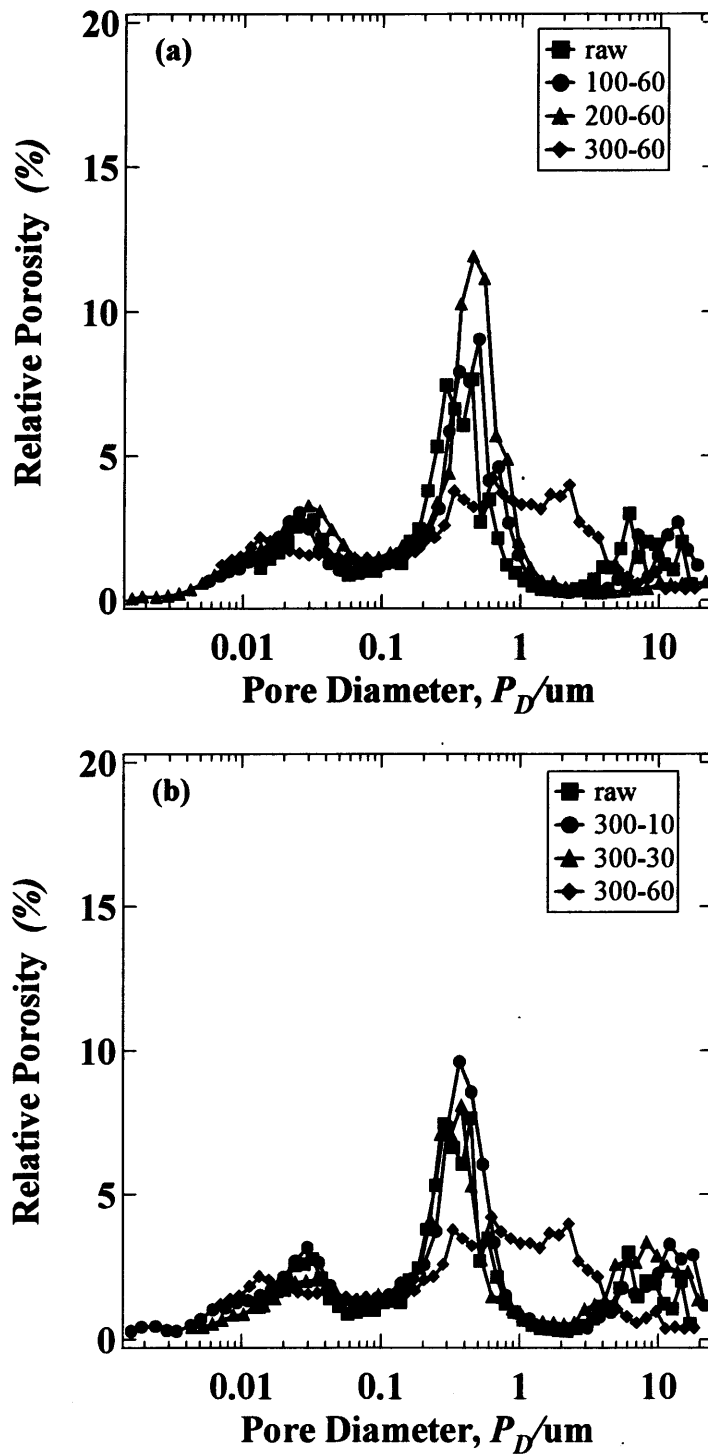
Figure 5.9 Relative porosity on pore size distribution of solidified porous ceramics at different

mechano-chemical treatments; (a) rotation speed, (b) milling time

Figure 5.10 shows the SEM images with inset image of the cross section of BPSA at different mechano-chemical treatment. In case of SEM images, it was somehow different to verify the change of surface area, microstructural, morphology, and powder particle size distribution through mechano-chemical treatment from these SEM images. On the other hand, we can observe holes and pore in the cross section images. A lot of holes were observed in raw powder. After mechano-chemical treated powder, it can be produced the porosity and pore structure. From these results, we can control the porous structure of non-firing ceramics by mechano-chemical treatment.

The mechanical strength of porous ceramics can be observed in Figure 5.11 that the bending strength also increases with mechano-chemical treatment. It can be ascribe the relationship between elution behavior and mechanical strength that the leaching of Al^{3+} and Si^{4+} measured by ICP analysis transform to new bonding leading to stronger mechanical strength with mechano-chemical treatment.
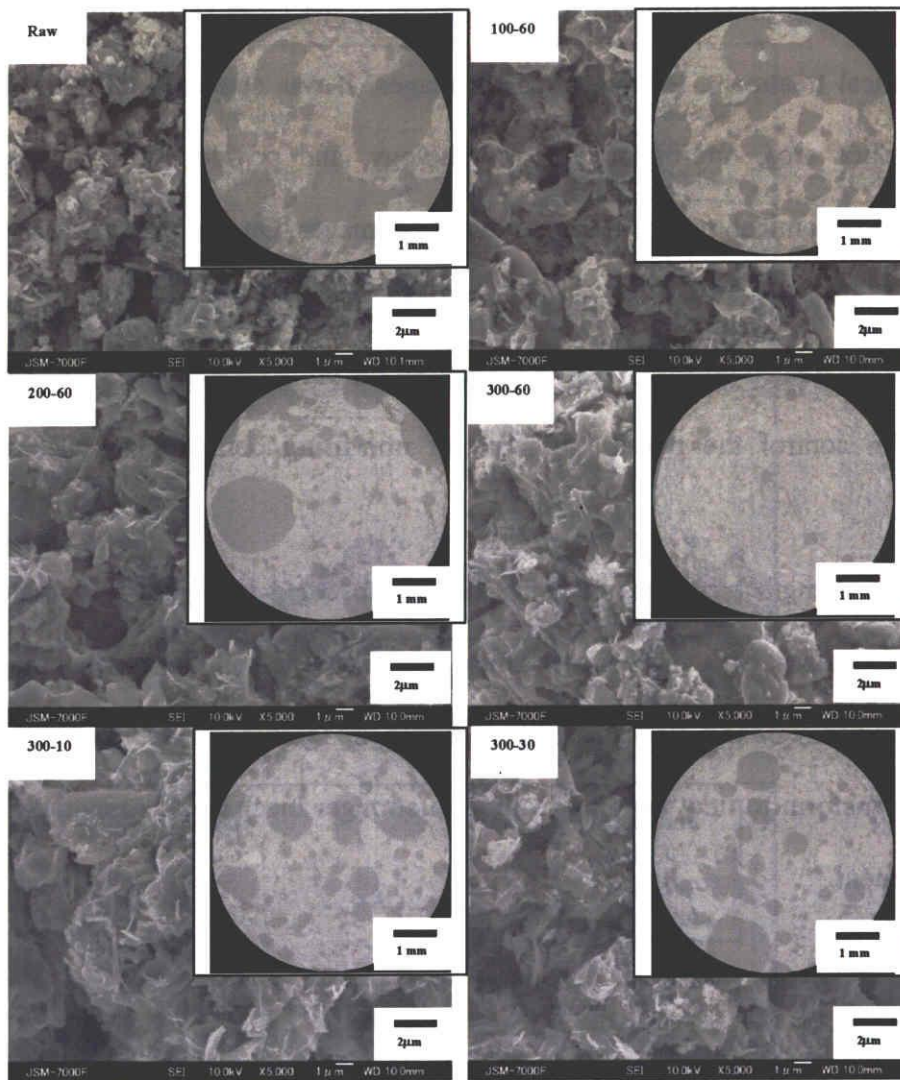
Figure 5.10 SEM photographs and cross section fabricated from BPSA at different mechano-

chemical treatments.
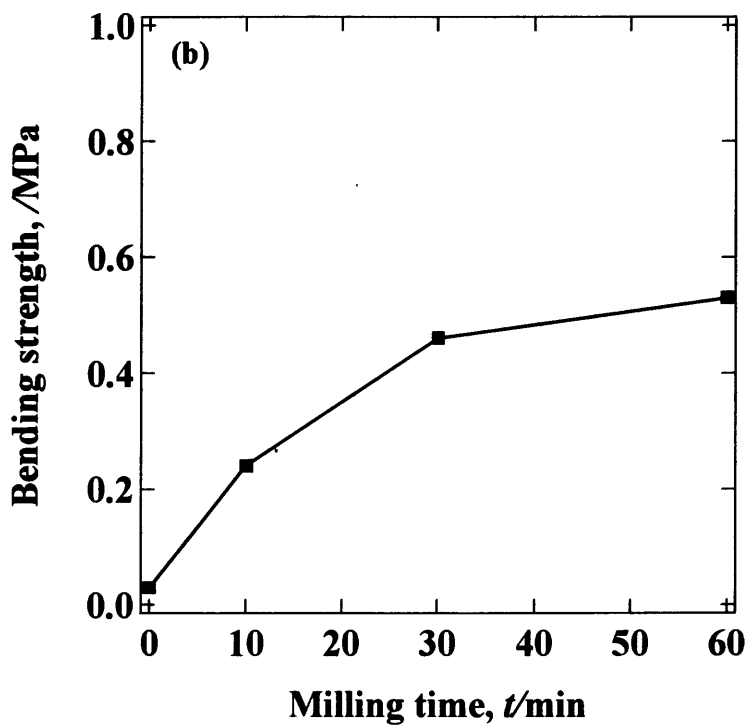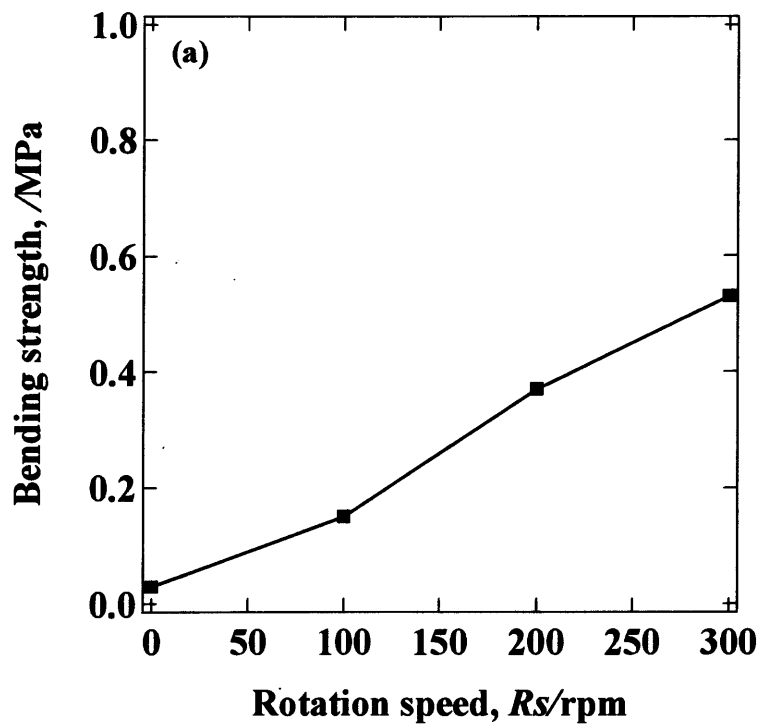
Figure 5.11 Mechanical strength of solidified porous ceramics at different mechano-chemical

treatments; (a) rotation speed, (b) milling time

5.2.4 Conclusion

A novel method to fabricate porous ceramics from waste materials with controllable properties using mechanochemically assisted chemical solidification was successfully developed. Base on our investigation, there is application mechano-chemical treatment into material which would be active surface of starting material. This result is attributed to the control porous property of solidified porous ceramics via mechano-chemical treatment. The porosity, pore diameter and mechanical strength of solidified porous ceramics are improved by mechano-chemical treatment. Its practical application needs optimization, which will be a subject of our further studies.

REFERENCES

[1] T. Banno, Y. Yamada and H. Nagae, Fabrication of porous alumina ceramics by simultaneous thermal gas generating and thermal slurry solidification. J. Ceram. Soc. Jap., 117 (2009) 713-716.

[2]A. Kritikaki and A. Tsetsekou, Fabrication of porous alumina ceramics from powder mixture with sol-gel derived nanometer alumina: Effect of mixing method. J. Eur. Ceram. Soc., 29 (2009) 1603-1611.

[3] T. Kojima, T. Fukai, N. Uekawa and K. Kakegawa, Fabrication of porous alumina using anisotropic boehmite particles. J. Ceram. Soc. Jap., 116 (2008) 1241-1243

[4] K. Adachi, M. Fuji and M. Takahashi, Fabrication of porous construction ceramics by gel casting of waste resources. Mat. Proc. Prop. Perf., 2 (2004) 219-225.

[5] D. Chakravarty and H. Ramesh and T.N. Rao, High strength porous alumina by spark plasma sintering. J. Eur. Ceram. Soc., 29 (2009) 1361-1369.

[6] M. Vlasova, G. D. Patino, N. Kakazey, M. D. Patino, D. J-Romero and Y. E. Mendez, Structural-phase transformations in bentonite after acid treatment Sci. Sin., 35 (2003) 155-166.

[7] T. Fukasawa, Z.-Y. Deng, M. Ando, T. Ohji and Y. Goto, Uniformly porous composites with 3-D network structure (UPC-3D) for high-temperature filter applications. J. Mat. Sci., 36 (2001) 2523-2527.

[8] K. Maca, P. Dobsak and A.R. Boccaccini, Fabrication of graded porous ceramics using alumina-carbon powder mixtures. Ceram. Inter., 27 (2001) 577-584.

[9] M. Vlahovic, S. Martinovic, P. Jovinic, T. Boljanac and V. Vidojkovi, P. Eur. Con. Chem. Eng., (2007) 1-6.

[10] W. K. W. Lee and J. S. J. van Deventer, Chemical interactions between siliceous aggregates and low-Ca alkali-activated cements. Cem. Con. Res., 37 (2007) 844-855.

[11] M. S. Yildirim, Y. Bicer and C. Yildiz, Utilization fly ash and polyproprelene. J. Poro. Mat., 3 (1996) 189-191.

[12] Y. Kim, J. H. Kim, K. G. Lee, S. G. Kang, Recycling of dust wastes as light weight aggregates. J. Ceram. Proc. Res., 6 (2005) 91-94.

[13] N. M. Al-Akhras and M. M. Smadi, Properties of tire rubber ash motar. Cem. Con. Com., 26 (2004) 821-826.

[14] H. Teng, Y.-C. Lin, and L.-Y. Hsu, Production of activated carbons from pyrolysis of waste tires impregnated with potassium hydroxide. J. Air & Was Man Assoc., 50 (2000) 1940-1946.

[15] David R. Waldbaum, Amer. Min., 50 (1965) 186-195.

[16] J. J. Ague, J. metamorphic Geol., 13 (1995) 299-314.

[17] A. Eiad-ua. T. Shirai, H. Watanabe, M. Fuji, K. Orito and M. Takahashi, Fabrication of non-firing ceramics assisted by particle surface activation using a planetary ball mill. Cer. Trans., 219 (2010) 129-135.

VI. CONCLUDING REMARKS AND POTENTIAL DIRECTIONS FOR

FURTHER RESEARCH

6.1 Concluding remarks

In chapter 2 The results presented in this thesis show that the techniques developed and used in this study are well suited for the investigation of the influence of mechano-chemical parameters on the interface surface of particles and properties of activated powder as well as on the milling energy values. Further detailed conclusions from the investigation of the influence of mechano-chemical variables on the activation of alumina are:

- As the rotation speed, milling time and diameter of ball increase, the line broadening increases and integral intensity decreases. The lattice and unit cell volume of alumina expanded during mechano-chemical activation.

- From the Williamson-Hall plots, it was understood that strain and size contributions exist simultaneously in the activated powders.

- The use of higher speed, prolonged milling and larger diameter of ball lead to higher specific surface area, X-ray amorphous material, physical broadening microstrain, smaller crystallites size and mean particle size distribution.

- Agglomerates during mechano-chemical treatment are formed rapidly in planetary ball mill for higher media surface (diameter of ball).

- Increasing the BPR also reduces the milling duration or rotation speed required for the activate surface of powder or the formation of new material.

- Mechanical strength of ceramic green body can be improved by mecahno-chemical treatment.

In chapter 3 Ceramic green body of alumina-silica composites has been prepared with wide range of Al_2O_3-SiO_2 ratio by mechanochemically assisted chemical solidification. A milling process for obtaining activated ceramic powder having mechanochemically amorphized surfaces by milling ceramic powder. An alkali treatment process was obtaining a ceramic green body by adding alkali water solution. Mechano-chemical treatment of alumina-silica composites is found to promote Al-O-Si bonding between alumina and silica components. New bonding or new composition formed at a high silica content range. Mechano-chemical treatment could provide a useful technique for synthesis alumina-silica composites which can be obtained from cheap raw materials.

In chapter 4 Non-firing ceramic from paper sludge ash was successfully fabricated by mechano-chemical with alkaline-chemical reaction process. The mechano-chemical treatment of planetary ball mill affects the fabrication of non-firing ceramics when the rotational speed, treatment time and diameter of balls were varied. The alkaline solution was used as a binder between ceramic particles forming a strong ceramic green body at room temperature. The chemical reaction depends on several factors such as the particle size distribution and mineral composition of paper sludge ash, kinds and concentration of the activator, reaction time, reaction temperature, etc. This process has an attractive route for shaping waste materials into valuable ceramics without firing process.

In chapter 5 Porous ceramics were successfully fabricated from black paper sludge ash by non-firing process. The composition of tire and waste material in black paper sludge ash was studied. It was confirmed that the addition tire ash influenced the gas generating in slurry. The mechano-chemical treatment with alkaline activation was used as a chemical synthesis of ceramic particles

to form porous structure of solidified specimen by gas generating. This fabrication technique has an attractive route for shaping waste material into valuable porous ceramics without conventional firing process. This research work demonstrated an easy method to control pore size of porous ceramics utilizing waste materials (BPSA).

6.2 Further research

- Further experiments and research are recommended to explore the effect of other mechano-chemical variables such as ratio between balls to powder, mode of milling (dry and wet) and etc through an experimental design which provide some advantageous to the conventional methods.

- More investigation of the effect of various defects formed during mechano-chemical activation on the reactivity of the minerals are now only at the beginning of their development.

- Application mechano-chemical treatment for the waste material to reduce cost of raw material and friendly to the environment.